Steven G. Boxer
Stanford University
Stanford, California

8 Photosynthetic Reaction Center Spectroscopy and Electron Transfer Dynamics in Applied Electric Fields

I. Overview

The movement of charge is central to photosynthetic function, including the charge displacement associated with photoexcitation of interacting pigments such as the special pair in the reaction center (RC), productive forward and wasteful back electron-transfer reactions, and proton uptake and release. Each of these steps generates or consumes a pair of charges and, consequently, an electric dipole moment, whose energy can be manipulated with external electric fields. An important example of an external electric field is the transmembrane potential generated by electron-transfer reactions and associated proton movement. Because the transmembrane potential is a vectorial property and the dipole moments within the photosynthetic unit have unique orientations relative to the direction of the transmembrane potential, the potential can have a significant effect on the energies of dipoles and consequently on the rates of various steps in photosynthesis. Therefore, in addition to being a very useful probe of the mechanisms of photosynthetic reac-

THE PHOTOSYNTHETIC REACTION CENTER, Volume II

tions, electric fields may play a significant physiological role in regulating various aspects of photosynthesis.

The structural, chemical, kinetic, and spectroscopic details of photosynthetic RCs are described elsewhere in this volume. A schematic view of the reactive groups that are the primary focus of this chapter is shown in Fig. 1, derived from the X-ray structure coordinates (Deisenhofer *et al.*, 1984,1985; Allen *et al.*, 1987; Chang *et al.*, 1991). The abbreviations used are P for the primary electron donor, a closely associated pair of bacteriochlorophylls (Bchls); B for the bridging or accessory monomeric Bchls; H for the bacteriopheophytins (Bphes); and Q for the quinone electron acceptors. As illustrated in Fig. 1, the initial electron transfer occurs predominantly along the chain of redox-active chromophores on the right side, denoted the L or A side chromophores; the chromophores on the left side are denoted the M or B side chromophores. The subscripts will not be needed in most of our discussion and are dropped.

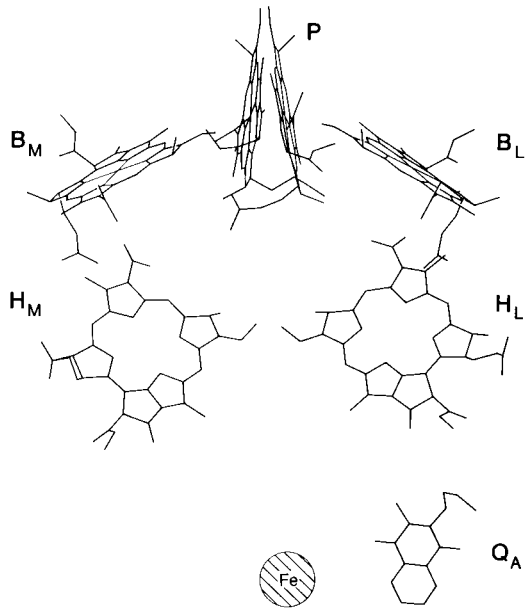

FIGURE 1 Arrangement of the chromophores in the RC taken from the X-ray coordinates for *Rps. viridis* RCs (Deisenhofer *et al.*, 1984,1985). A nearly identical figure is obtained for *Rb. sphaeroides* (Allen *et al.*, 1987; Chang *et al.*, 1991), except that ubiquinone replaces menaquinone (Q_A). P is a dimer of bacteriochlorophyll molecules. B_M and B_L are bacteriochlorophyll monomers; H_M and H_L are bacteriopheophytins. An approximate C_2 symmetry axis is directed along a vertical line that runs from the geometric center of P to the non-heme iron atom.

II. Technical aspects

A. Sample preparation

In the following section, some of the technical aspects and requirements for performing measurements in applied electric fields are discussed. Results of such measurements are discussed in subsequent sections. In this chapter, we consider primarily the application of external electric fields to samples of isolated RCs that are oriented randomly relative to the applied field direction. Ideally, experiments should be performed on single crystals; however, no data of this type have yet been reported for photosynthetic systems. Effects of applied electric fields have been measured for RCs in planar lipid bilayers, in Langmuir-Blodgett (LB) films, in poly(vinyl)alcohol (PVA) films, and in frozen glycerol/buffer glasses. Each system has advantages and disadvantages, so a summary may be useful for readers who have not used these techniques. Important related experiments on more complex systems by Trissl and coworkers (1987a,b), Vos and van Gorkom (1988), Vos (1988), and Dau and Sauer (1992) will not be reviewed further.

The $P^+Q_A^-$ recombination reaction has been studied in planar lipid bilayers (Gopher *et al.*, 1985; Feher *et al.*, 1988), which provide a good approximation of the native environment in the photosynthetic membrane. The applied field is generated by changing the potential of the solutions separated by the bilayer. Although this bulk transmembrane potential is known accurately, the actual field experienced by the RCs embedded in the bilayer is less well known, as discussed in detail by Feher *et al.* (1988). Issues include the precise position of the RC relative to the bilayer surfaces, the homogeneity of this position, and possible screening effects due to the electrical double layer at the surface of the bilayer. Both orientations of the RC director are present, which has been overcome cleverly by adding cytochrome *c* and reductant to one side of the bilayer and illuminating, thereby trapping those RCs in a non-electrogenic state with H_L reduced. Photocurrents then can be measured for the remaining fully functional and uniquely oriented population. Photocurrent measurements have the advantage of being exquisitely sensitive; the signal is not complicated by the effect of the applied field on the absorption spectrum (see subsequent text). Since the solutions must be fluid, the temperature can be varied over only a very limited range.

RCs have been inserted into LB films sandwiched between electrodes (Popovic *et al.*, 1985,1986a,b). Electric field effect measurements can be made either optically or electrically. This approach offers the advantage that the sample is oriented. As with the bilayer sample, typically both orientations are present; however, removing one population in the LB film is less straightforward. Detailed studies of the properties of these films (Alegria and Dutton, 1991a,b) demonstrate that films containing the detergent lauryl

dimethylamine-*N*-oxide (LDAO) exhibit considerable disorder. Also, when more than ~30 monolayers are assembled, the disorder, assessed by linear dichroism, increases considerably. Given this characterization, whether the electric field effect data reported earlier (Popovic *et al.,* 1985,1986a,b) were actually for highly oriented RCs is not clear. In contrast to planar lipid bilayers, LB films are very well suited to optical experiments on any time scale and the sample temperature can be varied at will. The hydration state of the LB after overcoating with electrodes has not yet been well characterized. In the electric field effect work reported to date, the sample thickness was estimated from the sample capacitance with an assumed dielectric constant. Consequently, the magnitude of the applied field (applied voltage divided by sample thickness) may not be very certain. This uncertainty appears to be better understood with the newer films (Alegria and Dutton, 1991a,b). Characterization of the defect density and charge injection have not yet been reported for LB films containing RCs, but these have been analyzed for simpler systems and shown to present problems (see, e.g., Vincett and Roberts, 1980). For both bilayer and LB samples, the RC director axis is expected to coincide approximately with the local C_2 axis of symmetry, and the applied field direction is approximately parallel to this direction. Therefore, dipoles on the L and M sides of the RC cannot be distinguished. (They have approximately the same projection on the local C_2 axis.) Some dipole moments of interest may be nearly perpendicular to the applied field direction.

Most of the spectroscopic data in applied electric fields has been for randomly oriented samples. The first generation of measurements was made using PVA films. The RCs are dissolved in a PVA solution, which is poured onto a glass slide. Typical thicknesses are 20 - 100 μm and can be measured with a precision caliper. The electrodes can be applied by attaching electrode-coated slides to the film with epoxy (Lösche *et al.,* 1987,1988), by metal vapor deposition (Lockhart and Boxer, 1987a,b,1988a), and by using wire mesh (DiMagno *et al.,* 1990). It is quite difficult to epoxy slides onto films without leaving air gaps. Metal vapor deposition requires that the sample be very dry because the deposition is done at high vacuum. The potential for thermal as well as photochemical damage during the deposition exists (the latter from the glowing filament used to vaporize the metal). Details of the use of wire mesh have not been given, but this appears to be a useful alternative. It is also possible to make very thin (several micrometers, measured using a thickness-measuring instrument such as a Sloan Dectak, accuracy ± 100 Å) PVA films by spin-coating the PVA onto a glass surface coated with one electrode, followed by vapor deposition of the second electrode. The advantage of using PVA samples is that very large electric fields can be applied, typically 1 MV/cm in thick films with DC fields and as high as 3 MV/cm for very thin, dry films using pulsed fields. In general, the highest fields are obtained at low temperature and for samples in vacuum.

Using PVA films has many disadvantages. The RC sample may become

somewhat oriented during the pouring of the film, although no evidence has been found for this occurrence in the electroabsorption measurements reported to date. Some sample degradation may occur. For measurements such as electroabsorption and most transient kinetic studies, which are sensitive to the bulk of the sample, degradation is not a severe problem; however, it may be a problem for fluorescence experiments. Absorption linewidths in PVA are considerably broader than in solution or in frozen glasses. This broadness can be a significant shortcoming for electroabsorption because the spectra involve first and/or second derivatives of the absorption spectra (see next section). As described in Section IV,C, prolonged irradiation leads to systematic changes in RC properties in PVA at low temperature.

We have shown that excellent electric-field-modulated absorption and fluorescence data can be obtained in frozen glycerol/buffer glasses (Hammes *et al.*, 1990; Schenck *et al.*, 1990; Middendorf, 1991; Middendorf *et al.*, 1991). A typical sample arrangement, which also defines the notation used in the following discussion, is shown in Fig. 2. The sample cell consists simply of electrode-coated glass or quartz slides held apart by an insulating spacer. The electrodes are either thin films of metal (typically about 80 Å of Ni) or indium-tin-oxide (ITO). Obviously, such samples are limited to temperatures at which the solvent is solid. The sample is not expected to become oriented and is fully hydrated. Typically, the absorption line shape is considerably narrower than in PVA films, so much more detail is observed in the absorption and electroabsorption spectra and higher quality absorption spectra, needed for the quantitative analysis of electroabsorption spectra (see Section III,A), are obtained more easily. Another advantage of working in frozen glasses is

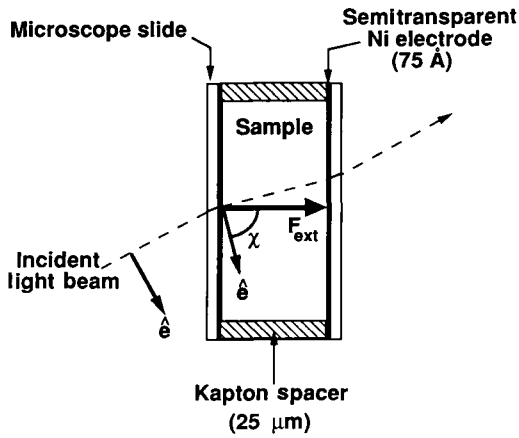

FIGURE 2 Typical sample cell configuration for measuring electromodulation spectra in frozen glasses. The semitransparent electrodes are connected to a high voltage power supply.

that the sample conditions prior to freezing can be adjusted as desired. Thus, it is possible to trap intermediates or perform titrations, then measure the electroabsorption spectrum. We have extended the measurements to 1.5 K using frozen glycerol/buffer glasses (Middendorf, 1991; Middendorf *et al.,* 1991; Middendorf *et al.,* 1993). Very small quantities of sample are required, experiments can be performed immediately on isolation (important for some unstable mutants), and the sample can be recovered. One drawback is that the maximum applied field is considerable lower in frozen glasses than in PVA films, with a maximum around 0.5 MV/cm. For reasons that are not fully understood, samples containing ionic detergents (e.g., LDS or SDS) exhibit very large wavelength-dependent field-induced modulation of the transmission, likely due to modulation of the refractive index of the sample (Gottfried *et al.,* 1991b). This effect obscures even the strongest electroabsorption signal.

B. Apparatus

Details of the apparatus used for measuring absorption and emission spectra in fields have been described elsewhere (Gottfried, 1990; Oh, 1991). Commercial power supplies with a fast rise time can be used to amplify the voltage of an input waveform. For electromodulation spectroscopy, a reasonably inexpensive, high quality supply has been designed by Joe Rolfe at Stanford University (schematics are available). The field is modulated sinusoidally, and the signal is detected at the second harmonic of the field modulation frequency using a lock-in amplifier. For measurements of kinetics, it is often most useful to measure effects using time-gated fields. This procedure offers two advantages. First, it is possible to generate larger fields without sample breakdown. Semitransparent electrodes have a considerable resistance, and the sample RC time constant limits the rate at which fields can be applied and removed (typical time constants are on the order of 10 μs for samples several μm thick and a few mm^2 in area with ITO electrodes). Second, in many experiments it is interesting to control the timing of the flash excitation, electric field (amplitude and sign), and probe beam (Section IV,D). All these elements can be controlled by a central timing interface, leading to many new types of experiments under automated control, not unlike the function of a modern NMR spectrometer.

A wide variety of detectors has been used. Solid state detectors such as PIN, Si avalanche, or Ge photodiodes work very well. These detectors are especially useful for studies of RCs because Si is sensitive to about 1100 nm (Ge is sensitive to about 1600 nm). Typical photomultiplier tubes offer excellent amplification, but are far too noisy for electroabsorption spectroscopy. For studies in the ultraviolet range, we use a UV-sensitive photomultiplier with voltage applied across only a few dynodes. Extensions into the mid-IR are in progress.

III. Electroabsorption (Stark effect) spectroscopy

A. Principles

The measurement of the effect of an applied field on an absorption line shape was developed first by Stark and Lo Surdo (1913). The name "Stark effect" is widely used to describe the effect of an applied electric field on many physical processes; however, the expressions electroabsorption, electromodulation, and electrochromism also have been used. We will use electroabsorption because this term is most descriptive. Although the technique was applied extensively to simple organic molecules in the 1970s (Hochstrasser, 1973; Liptay, 1974), surprisingly little application has been made to complex organic and inorganic molecules or molecules of biological interest. This lack of use appears to be the result of the (mistaken) impression that the experiments are difficult to perform. Prior to the work on RCs, only one study had been done on a biological system, a very interesting study of bacteriorhodopsin by Mathies and Stryer (1976), in which it was demonstrated that photoexcitation of the retinal chromophore involves a very large change in dipole moment (about 15D). Some work has been reported for isolated porphyrins (Malley, 1967; Davidsson, 1980,1983; Davidsson and Nordén, 1977) and polyenes (Ponder and Mathies, 1983; Liptay *et al.,* 1988).

Much of the pioneering electroabsorption spectroscopy was developed by Liptay (Liptay and Czekalla, 1960; Liptay, 1974) and Labhart (1961). Most of Liptay's work has been done in fluid solution. This set-up offers the advantage that information can be obtained on ground state dipole moments (due to reorientation of the molecule in the field leading to dichroism); however, it also complicates the analysis and experimental method. By working with molecules immobilized in a polymer film or frozen glass, much higher quality data can be obtained because much higher fields can be applied. The analysis is considerably simpler, because information is obtained on differences between properties of the ground and excited state. As will be seen in the next section, even in solid solution it is often quite difficult to extract reliable electro-optic parameters.

The theory of electric field effects on molecular spectra has been developed in detail (Liptay and Czekalla, 1960; Labhart, 1961; Mathies, 1974). For an isotropic immobilized sample, the line shape of the field-induced absorbance change (ΔA) can be described by a sum of the zeroeth, first, and second derivatives of the absorption spectrum [$A(\nu)$]:

$$\Delta A(\nu) = (f \cdot \mathbf{F}_{ext})^2 \left\{ A_\chi A(\nu) + \frac{B_\chi}{15hc} \frac{\nu d[A(\nu)/\nu]}{d\nu} + \frac{C_\chi}{30h^2c^2} \frac{\nu d^2[A(\nu)/\nu]}{d\nu^2} \right\} \quad (1)$$

where ν is energy in wavenumbers, h is Planck's constant, and c is the speed of light. The local field correction factor f relates the magnitude of the field present at the chromophore, $\mathbf{F}_{int}$, to that of the externally applied field: $\mathbf{F}_{int} = f \cdot \mathbf{F}_{ext}$. In general, f is a tensor quality; however, we will treat it as a scaler for simplicity (Böttcher, 1973). The value of f is not known accurately, but is likely between 1.0 and 1.3 for most systems described here (Lockhart and Boxer, 1987a,b; Lösche *et al.*, 1987). Lack of knowledge of this factor limits the absolute accuracy of the values of electro-optic parameters derived from electroabsorption measurements. In frozen solution, the solvent-to-solvent variation in f is likely to be quite small. We have found little quantitative difference in solvents ranging from frozen toluene to water for molecules that are soluble in a wide range of solvents. For the most part, we are concerned with comparisons of the properties of different chromophores under roughly comparable conditions, so the limitation is not so serious; however, significant variations in f might exist in the organized environments surrounding biological chromophores. Parameter values obtained from experimental data are reported assuming $\mathbf{F}_{int} = \mathbf{F}_{ext}$ divided by f, to explicitly separate experimental error from uncertainties in the value of f.

The coefficients A_χ, B_χ, and C_χ depend on molecular parameters such as the transition polarizability and hyperpolarizability, and the differences in polarizability ($\Delta\boldsymbol{\alpha}$) and permanent dipole moment ($\Delta\boldsymbol{\mu}_A$) between the ground and excited electronic states connected by the optical transition that is being probed. In particular, the coefficient C_χ for the second derivative component is related to $\Delta\boldsymbol{\mu}_A$ as:

$$C_\chi = |\Delta\boldsymbol{\mu}_A|^2\left[5 + (3\cos^2\chi - 1)(3\cos^2\zeta_A - 1)\right] \qquad (2)$$

where χ is the experimental angle between the electric vector of the probing polarized light and the direction of the applied electric field (see Fig. 2), and ζ_A is a molecular angle between $\Delta\boldsymbol{\mu}_A$ and the transition moment. By measuring ΔA as a function of the experimental angle χ using a polarized probe beam, the angle ζ_A can be determined very accurately unless absorption bands overlap. (Examples of such curves for various values of ζ_A are shown with data in Fig. 5.) Note that for $\chi = 54.7°$ (the magic angle), $C(\chi = 54.7°) = 5|\Delta\boldsymbol{\mu}_A|^2$, that is, the dependence of ΔA on ζ_A vanishes.

If contributions from the transition polarizability are neglected, the B_χ term in Eq. 1 can be expressed as (Mathies, 1974):

$$B_\chi = \frac{1}{2}\{5\mathrm{Tr}(\Delta\boldsymbol{\alpha}) + (3\cos^2\chi - 1)[3(\mathbf{p}\cdot\Delta\boldsymbol{\alpha}\cdot\mathbf{p}) - \mathrm{Tr}(\Delta\boldsymbol{\alpha})]\} \qquad (3)$$

where $\mathbf{p}$ is a unit vector in the direction of the transition dipole moment. The magnitude of B_χ, and therefore the value of $\mathrm{Tr}(\Delta\boldsymbol{\alpha})$ deduced from the analy-

sis, depends on the orientation and relative magnitudes of the components of the $\Delta\alpha$ tensor through the $\mathbf{p} \cdot \Delta\alpha \cdot \mathbf{p}$ term. This quantity can be determined by measuring the χ dependence of the first derivative contribution to the electroabsorption spectrum.

Equation 1 applies equally well to emission (fluorescence or phosphorescence) as absorption, except that a factor of ν^3 replaces ν in front of the derivatives. If absorption and emission involve the same electronic states, the magnitude and line shape of the effects are expected to be comparable. Often, however, electric-field-dependent processes occur during the excited state lifetime, which can modify drastically the emission line shape predicted by the formalism just presented (Lockhart *et al.,* 1991).

In general, it proves to be much more difficult to obtain very high quality absorption spectra than electroabsorption spectra. To analyze ΔA data, one needs high quality first and second derivatives of the absorption spectrum obtained under identical conditions. For this purpose, great care must be taken to obtain a true baseline (i.e., the zero of absorbance and ΔA must be known accurately). Data for which the baseline is adjusted arbitrarily or for which ΔA does not return to zero far from an absorption band should be viewed with caution. Such baseline offsets can distort measurements of the χ dependence of ΔA severely as well. Finally, even assuming that the formalism in Eq. 1 is valid, if absorption bands overlap, it may be very difficult to obtain quantitative information from electroabsorption spectra, because ΔA can be both positive and negative, leading to partial cancellation of overlapping bands. [This effect also can distort measurements greatly as a function of χ, which are best done for the entire spectral line shape (Oh, 1991).] The best strategy is to obtain spectra under conditions in which the bands are narrowest, thus minimizing this problem.

The quantitative analysis of the Stark effect spectrum in terms of the derivatives of the absorption spectrum can be accomplished by several procedures. The most commonly used method is to fit the absorption band(s) of interest to a sum of Gaussian or higher order Gaussian functions. Given enough components, this procedure can lead to an essentially perfect fit to the absorption spectrum within the signal-to-noise and is the equivalent of a smoothing procedure. The components in the best fit have no physical meaning. The derivatives of the best fit can then be obtained, and these derivatives are fit to the $\Delta A(\nu)$ spectrum using a least-squares algorithm to obtain the contributions from each derivative. A related, but superior procedure has recently been introduced (Middendorf *et al.,* 1993). In this method the absorption and Stark spectra are fit *simultaneously,* with the calculated deviation χ^2 for each spectrum weighted equally during minimization. The rationale behind this approach is that small errors in the measurement of the absorption spectrum will be amplified enormously in the derivative spectra, and thus small increases in χ^2 for the absorption fit may be offset by a better fit to the Stark spectra.

B. Bacterial reaction centers

The first report of the electroabsorption spectrum for a photosynthetic system appeared in an abstract (DeLeeuv *et al.*, 1982). Even at a qualitative level, it was apparent that the lowest Q_Y transition of the special pair is much more sensitive to an applied field than that of the monomer Bchl and Bphe bands. We reported measurements at room temperature in PVA with a focus on the χ dependence of the effect, giving the first information on ζ_A (Lockhart and Boxer, 1987a,b); this report soon was followed by work from Feher's (Lösche *et al.*, 1987,1988) and our group (Boxer *et al.*, 1987; Lockhart and Boxer, 1988a) at 77 K in PVA films. We also studied the properties of the isolated pigments for comparison with the results from proteins and the Q_X and Soret regions of the spectrum (Lockhart and Boxer, 1988a). The spectrum of methylbacteriopheophorbide a (Bphe where a methyl replaces the phytyl ester) throughout the visible and NIR regions is shown in Fig. 3 (Gottfried and Boxer, 1991). ΔA is approximated well by the second derivative of the absorption band for the Q_Y transition; including the measured angle dependence of ΔA gives values of $\zeta_A = 16.9 \pm 2°$ and $|\Delta\boldsymbol{\mu}_A| = 2.0 \pm 0.1$ D/*f* for the origin band. The Q_X and Soret bands exhibit more complex line shapes, dominated by a first derivative contribution; however, the sensitivity of these bands to an applied field is much smaller than that of the Q_Y bands.

An electroabsorption spectrum of RCs in the Q_Y region in a glycerol/buffer glass at 1.5 K is shown in Fig. 4 (Middendorf *et al.*, 1991). As in the original PVA spectra, the enhanced sensitivity of the special pair Q_Y band to an applied field is evident. Angle dependent data in PVA at 77 K are shown in Fig. 5 (Lockhart *et al.*, 1988); similar but less accurate results (due to sample scatter) have been obtained in frozen glasses. A striking observation is that ζ_A is substantially larger for the special pair than for an isolated monomeric Bchl. Further, although ζ_A values for isolated monomeric Bchla and Bchlb are quite different, ζ_A for the P bands in *Rhodobacter sphaeroides* and *Rhodopseudomonas viridis* RCs (dimers of Bchla and Bchlb, respectively) are the same, within experimental error. Because the structures of P in the two species of RCs are quite similar, we suggested that the value of ζ_A is related in some way to the structure of the special pair. At this level of accuracy, the data are consistent with mixing with states whose dipole moments connect the centers of the macrocycles that constitute P (Lockhart and Boxer, 1988a). Of course, these data only define cones for which the angle between $\Delta\boldsymbol{\mu}_A$ and the transition moment is ζ_A. Because $|\Delta\boldsymbol{\mu}_A|$ is substantially larger for P than for the monomeric chromophores, it is reasonable that charge-transfer (CT) states on P or between P and B play a significant role. Irrespective of which states contribute, the key observation is that ζ_A is not $\sim 90°$ (Boxer *et al.*, 1989). Because the special pair has approximate C_2 symmetry, its electronic states should have C_2 symmetry and $\Delta\boldsymbol{\mu}_A$ should lie along the C_2 axis. In this case,

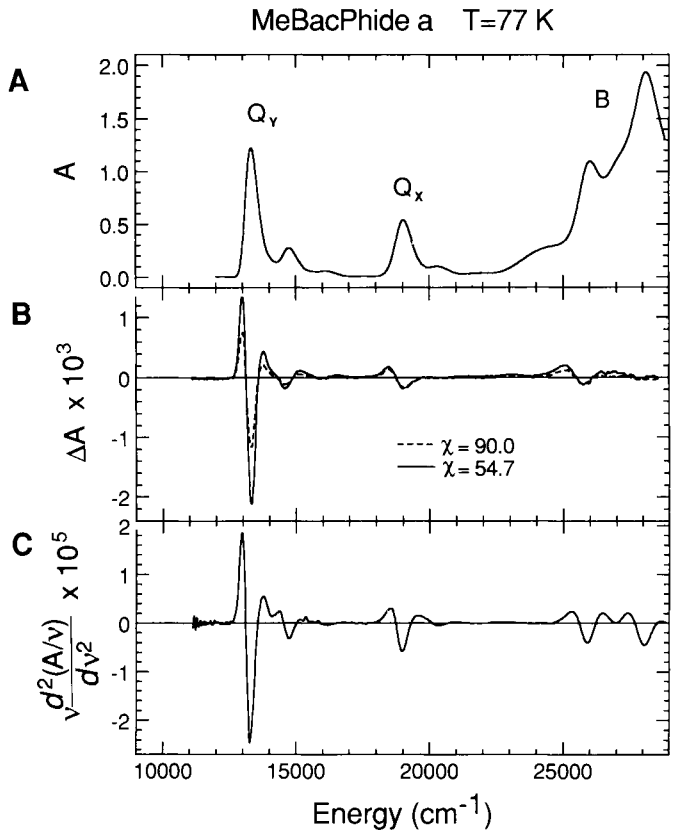

FIGURE 3 Absorption (A), electroabsorption (B), and second derivative (C) of absorption of monomeric methylbacteriopheophorbide a in polymethylmethacrylate (T = 77 K, F_{ext} = 5.36 × 10^5 V/cm) (Gottfried and Boxer, 1991). Electroabsorption spectra are shown for the experimental angles χ = 90° (---) and χ = 54.7° (magic angle) (—).

ζ_A should be approximately 90° because the Q_Y transition moment is approximately perpendicular to the local C_2 axis (Zinth *et al.*, 1985). This is not the case (Fig. 5); therefore, the electronic symmetry of ^1P is broken by some feature of the structure and environment of the special pair. Thus, not only is there a large displacement of charge on photoexcitation of the special pair, but this displacement breaks the local symmetry. It is tempting to speculate that this change may be related to unidirectional electron transfer.

Several limitations and problems are inherent in this basic interpretation. Nothing is known about the ground state dipole moment. Lacking any information, the ground state moment generally has been assumed to be small

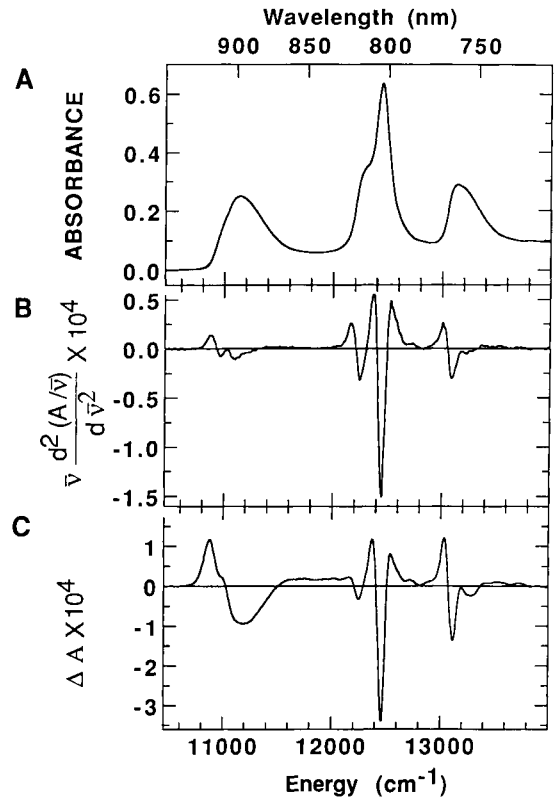

FIGURE 4 Absorption (A), second derivative of absorption (B), and electroabsorption (C) spectra in the Q_Y region of wild-type *Rb. sphaeroides* RCs in a 50% (v/v) glycerol/buffer glass at 1.5 K ($F_{ext} = 9.90 \times 10^4$ V/cm; $\chi = 90°$). From these spectra it is evident that the special pair absorption around 890 nm is much more sensitive to an applied field than are the monomer Bchls, which absorb around 800 nm, and that the electroabsorption lineshape for P is quite different from the second derivative of the absorption (Middendorf, 1991).

relative to that of ^{1}P, so $|\Delta\mu_A|$ is associated with ^{1}P. Plato and co-workers have suggested that the ground state dipole moment may be nonnegligible (Plato *et al.*, 1988). A second limitation is that the observables only define cones, so we do not know which end of the dipole is positive or negative. As discussed in Section IV,C, in principle, obtaining information on the absolute direction of the excited state dipole moment from an analysis of the fluorescence lineshape in an electric field is possible (Lockhart *et al.*, 1991). A third dilemma, pointed out by Scherer and Fischer (1986) well before the more quantitative data were available, is that a simple model invoking mixing with CT states to

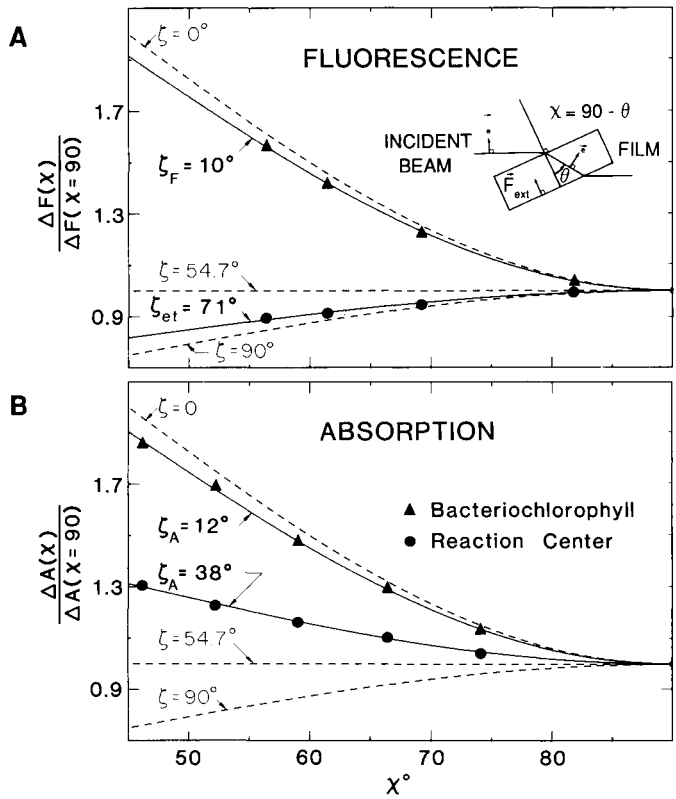

FIGURE 5 Comparison of the angle dependence of the fluorescence and absorption electric field effect for P (Lockhart *et al.*, 1988). A. The dependence of $\Delta F(\chi)/\Delta F(\chi = 90°)$ on the experimental angle χ for Q_A-depleted *Rb. sphaeroides* Rcs (●) and the dependence of $\Delta F(\chi)/\Delta F(\chi = 90°)$ on χ for six-coordinate bacteriochlorophyll a in polymethlmethacrylate (▲), in addition to the best fit of the data for each to Eq. 2 to obtain ζ_A. The observed internal angle ζ is seen to be very different for absorption and fluorescence, although the directions of the transition dipole moments are approximately parallel.

explain the large effect for P also leads to the prediction that the electroabsorption line shape should depend strongly on applied field. In PVA, we (Lockhart and Boxer, 1988a) showed that the line shape is insensitive to applied field strength over a wide range (this has recently been extended to nearly 3MV/cm by K-Q. Lao and S. G. Boxer, unpublished data). Our group and Feher's demonstrated that the effect scaled with the square of the applied field up to 1 MV/cm, as predicted by Eq. 1.

Although the line shape of the electroabsorption spectrum for the special pair Q_Y band in PVA films resembles the second derivative of the absorption,

very detailed comparisons reveal some discrepancies (Lösche *et al.*, 1987; Lockhart and Boxer, 1988a). By working in glycerol/buffer glasses, in which the inhomogeneous linewidth is considerably smaller than in PVA, the discrepancy becomes much more evident, as shown in Figs. 4 and 6. If the basic model described in Eq. 1 is assumed to be valid, then the data can be analyzed further to extract contributions from zeroeth and first derivative contributions, as discussed in detail by Middendorf *et al.* (1993). As shown in Fig. 6, a much better, although far from perfect, fit is obtained, which is not surprising because more parameters are involved. Even at a qualitative level, there appears to be a large first derivative contribution to ΔA, implying a large polarizability change. The fits give $\mathrm{Tr}(\Delta\alpha) \sim 900\ \text{Å}^3/f^2$, which is more than an order of magnitude larger than for a monomeric Bchl, in addition to a nontrivial zeroeth derivative contribution. Although only a very narrow range of applied fields was sampled at 1.5 K, no change in line shape was observed.

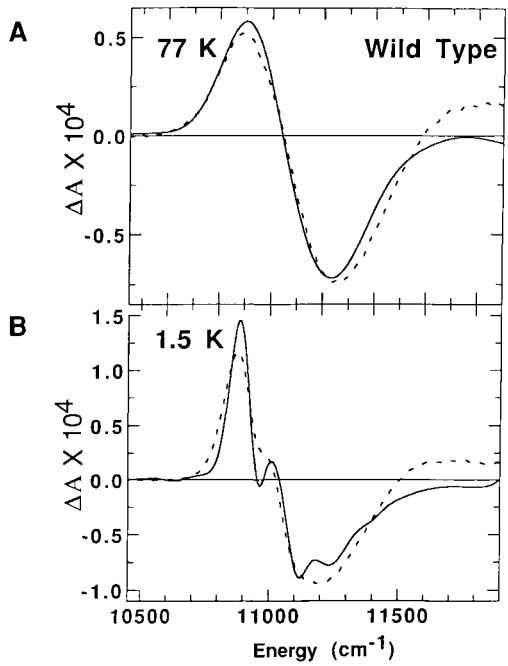

FIGURE 6 Expanded view of the experimental (---) and simulated (—) electroabsorption spectra of the special pair Q_Y band of wild-type *Rb. sphaeroides* RCs in 50% (v/v) glycerol/buffer at 77 K(A) and 1.5 K(B) (Middendorf, 1991). The greatly improved resolution at 1.5 K is evident. The spectra at 77 and 1.5 K were obtained on the same sample under otherwise identical conditions. The simulations include contributions from zeroeth, first, and second derivatives, since the second derivative alone does not fit the low temperature data very well (cf., Fig. 4). The first derivative contribution is large, corresponding to $\mathrm{Tr}(\Delta\alpha) \sim 900\ \text{Å}^3/f^2$ (see text).

On further consideration of these results, we suggest that ^1P should be highly polarizable. In the simplest one-electron Hückel model for a molecular dimer, CT states corresponding to movement of an electron from the highest occupied molecular orbital (HOMO) of one molecule to the lowest unoccupied molecular orbital (LUMO) of the other should be close in energy to the locally excited or exciton states of the dimer. This notion has been discussed using different terminology by many investigators (Scherer and Fischer, 1986; Parson and Warshel, 1987; Parson *et al.*, 1988,1989,1990; Won and Friesner, 1988a,b; Boxer *et al.*, 1989; Rodriguez and Holten, 1989; Thompson *et al.*, 1991). The actual location of CT states and the splitting between the states by the environment is a quantitative question that is far from resolved. The notion that nearby CT states mix strongly *implies* that the ^1P state should be highly polarizable; therefore, a substantial first derivative contribution to the electroabsorption line shape should be observable. As pointed out in the detailed treatment by Scherer and Fischer (1986), on application of an electric field, the energies of CT states must change and the ΔA line shape should depend on field strength. The data in Fig. 6 are consistent with a very large polarizability change; however, the predicted field-dependent line shape is not observed, at least not over the field range studied. These issues were discussed in detail earlier (Boxer *et al.*, 1989), prior to the availability of data in frozen glasses. Although various explanations could be provided, none was particularly satisfactory.

This puzzle led Middendorf *et al.* (1991,1993) to propose that the large observed dipole moment in ^1P is *induced* by a large asymmetric matrix electrostatic field in the RC. The idea is simply that a very polarizable chromophore is very sensitive to the environment and, because the environment around the special pair is organized, the constellation of polar, charged, and polarizable groups in the vicinity of P could induce the substantial observed dipole moment in ^1P. Ample precedent exists for this notion, both for simple polyenes, which are well known to be highly polarizable, even in disordered matrices (Liptay *et al.*, 1988) and for polyenes in antenna and RC complexes, as discussed in the next section (Gottfried *et al.*, 1991a,c). Provided the matrix electrostatic field is large compared with the externally applied field and provided the CT states are not too close in energy to the locally excited or exciton states, electroabsorption spectroscopy in the applied external field simply samples the matrix-induced dipole moment. The intrinsic molecular polarizability is still preserved, of course, and is observed also as a first derivative contribution to the electroabsorption line shape (see Fig. 6). If the energies of CT states are very close to the locally excited or exciton states, or if the applied field is very large, then a field-induced line shape change is predicted (Scherer and Fischer, 1986). Apparently, with the fields available to date ($\mathbf{F}_{ext} \sim 2$ MV/cm in PVA), this limit has not been reached. A more quantitative analysis is provided elsewhere (Middendorf *et al.*, 1993). One immediate implication is that the CT states are unlikely to be nearly resonant

with the exciton transitions, as has been suggested in some models (Won and Friesner, 1988a,b). If some more fundamental breakdown of the assumptions used to derive Eq. 1 occurs, then the mechanism proposed by Middendorf *et al.* (1993) may need to be revised further. For example Reimers and Hush (1991) have considered the possible complicating effects of vibronic coupling in the context of the analysis of electroabsorption data we have obtained for several transition metal complexes (Oh and Boxer, 1990; Oh *et al.*, 1991).

If correct, this model has several interesting implications. $|\Delta\boldsymbol{\mu}_A|$ and ζ_A are more a reflection of the magnitude and direction of the matrix field than of the direction of the dipole moment associated with the mixing of particular CT state(s) leading to the large polarizability. The essential implication remains that some environmental effect causes a marked deviation of the charge distribution in ^1P from the local C_2 axis. Most theorists have not discussed the molecular polarizability of ^1P explicitly. However, polarizability is likely to be important to understanding the optical and redox properties of the special pair. Electroabsorption data can serve as a stringent test for any theoretical treatment that claims to explain these properties. One treatment of the optical properties gave a small intrinsic dipole moment for ^1P (a reasonable result in light of this discussion) and suggested a role for the environment in determining the observed electroabsorption effects (Thompson *et al.*, 1991).

Several interesting RC mutants have been reported in which the spectral properties of the chromophores are perturbed substantially. These mutants include the heterodimer mutants in which one of the two Mg atoms in the Bchls composing the special pair appears to be absent (Bylina and Youvan, 1988; Kirmaier *et al.*, 1988), a mutant in which the H_L chromophore appears to retain Mg, that is, it is a Bchl (known as the β-mutant; Kirmaier *et al.*, 1991), a mutant in which H_L appears to be absent (known as the D_{LL} mutant; Breton *et al.*, 1990; Robles *et al.*, 1990a,b), and a series of mutants involving symmetrization of amino acid residues which make contact with the special pair (known as the pAT3 or SYM-1 mutants (Taguchi *et al.*, 1992; Stocker *et al.*, 1992).

DiMagno *et al.* (1990) and Hammes *et al.* (1990) reported data for the M side heterodimer mutant from *Rb. capsulatus* (M)H200L and *Rb. sphaeroides* (M)H202L, respectively. In both cases, a large low-energy electroabsorption feature was found, as illustrated in Fig. 7B. Assuming that the Bchl monomer band around 800 nm is unperturbed and can serve as an internal standard, the magnitude and linewidth of ΔA for the lowest energy feature are comparable to those for P in the wild-type; however, the absorption at that wavenumber is considerably weaker than for wild-type. Such data are more difficult to analyze than those for wild-type because it is not obvious, especially for samples in PVA and for *Rb. capsulatus,* how to evaluate the underlying

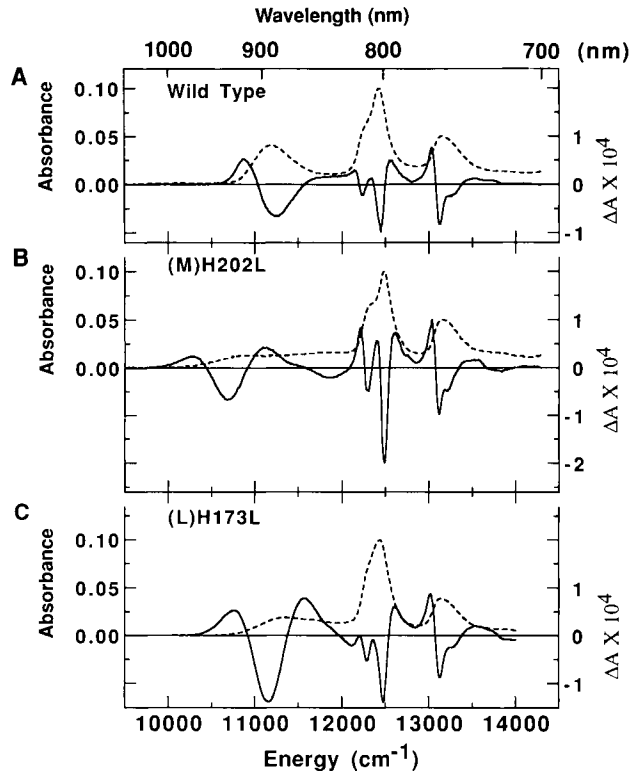

FIGURE 7 Absorption (---) and electroabsorption (—) spectra for *Rb. sphaeroides* wild-type (A), (M)H202L M-side heterodimer (B), and (L)H173L L-side heterodimer (C) in glycerol/buffer glasses at 77 K (Schenck *et al.*, 1990). The absorption spectra have been scaled to the same absorbance at the peak maximum around 800 nm; the electroabsorption spectra were scaled to the same applied field strength, so the magnitudes of ΔA can be compared directly. (Note that the resolution of two Bchl monomers at 800 nm varies slightly, thereby affecting the meaning of the scaling of absorption at the peak maximum to some extent.)

absorption. Fortunately, for *Rb. sphaeroides* in a frozen glycerol/buffer glass, some substructure is observed in the Q_Y region. Although the Q_Y band of the heterodimer often is described as featureless, at least two resolved bands are present. By fitting these bands with a simple sum of Gaussians, we obtained $|\Delta\mu_A|$ between 13 and 17 D which is several times larger than the value for wild-type. (No attempt was made to extract zeroeth and first derivative contributions, which are not obviously present.) Norris *et al.* (1990) initially deduced a very wide range of values (between 14 and 45 D) for the *Rb. capsulatus* heterodimer and described the ^1P state as essentially a

pure CT state. Later work gave only the lower limit ($|\Delta\mu_A| > 14$ D). For *Rb. sphaeroides,* the L side heterodimer (L)H173L has been prepared by Schenck and co-workers (1990) (Fig. 7C). The deduced value of $|\Delta\mu_A|$ likewise was found to be several times larger than for wild-type. The simplest interpretation of these data is that ^{1}P is more dipolar in the heterodimers than in the wild-type because the energy of the lowest-lying CT states that mix into the locally excited or exciton states is lower. [Bphe is easier to reduce than Bchl *in vitro* (Fajer *et al.,* 1975).] The unresolved quantitative issues are how much lower in energy these CT states are in the environment of the RC and whether essentially pure CT states are lower or higher in energy than the optically accessed transitions around 900 nm (McDowell *et al.,* 1991).

The absorption spectrum of the *Rb. sphaeroides* β-mutant (M)L214H (Kirmaier *et al.,* 1991) shows a loss of intensity in the 760-nm band associated with the Bphes. A well-resolved new band corresponding to β_L (Bchl in place of Bphe in the H_L site) is found at 780 nm at 77 K in a glass (Steffen, 1993). Interestingly, the intensity of the new 780-nm band is approximately the same as the remaining band at 760 nm (due to H_M), and it is much weaker than the 800-nm band corresponding to two monomeric Bchls. ΔA for the new 780-nm band is considerably larger than for the remaining 760-nm band. It is comparable in intensity to that for the band at 800 nm, although the absorbance at 780 nm is much smaller than that at 800 nm. We had noted early on that the lower energy member of the overlapping bands at 760 nm in the wild-type (assigned as H_L) is considerably more sensitive to an applied field than the higher energy member, and that it is more sensitive to an applied field than an isolated pure monomeric Bphe (Lockhart and Boxer, 1988a). Interestingly, this same pattern is preserved in the β-mutant, although Bphe H_L has been converted to a Bchl. Therefore, like the apparent reduction potential of β_L, which appears to be determined more by the site than by the chemical nature of the chromophore (Kirmaier *et al.,* 1991), both the oscillator strength and electroabsorption data seem to be determined by the site. The physical origin of these environmental effects is not yet understood. Recent data suggest that the dielectric constant in the vicinity of the H_L binding site is considerably larger than in the vicinity of H_M (Steffen, 1993).

The *Rb. capsulatus* D_{LL} mutant involves symmetrization of the lower two-thirds of the D helices and leads, remarkably, to loss of H_L (Robles *et al.,* 1990a,b). The electroabsorption spectrum is unremarkable, clearly demonstrating the loss of the more field-sensitive feature (H_L) on the low-energy side of the 760-nm band, with no evidence for new bands and minimal perturbation of the other features (J. W. Stocker and S. G. Boxer, unpublished observations; these spectra were obtained on whole chromatophore membranes in the absence of antenna complexes, for which obtaining absorption spectra and a reliable baseline is difficult). We have prepared a symmetry mutant involving the upper third of the D helix and a portion of the loop between the D and E helices [originally called the pAT3 mutant (Woodbury *et al.,* 1990)

and renamed SYM-1 (Taguchi *et al.*, 1992; Stocker *et al.*, 1992)]. SYM-1 and D_{LL} overlap at only one residue that differs between the L and M sequences, residue M195, which is phenylalanine in wild-type and is converted to histidine in the mutants. Remarkably, the special pairs in both SYM-1 (Taguchi *et al.*, 1992; Stocker *et al.*, 1992) and D_{LL} (J. Breton, personal communication) are considerably more difficult to oxidize, suggesting a significant role for residue M195 in determining the redox potential of P. Indeed, the site-specific mutant (M)F195H in *Rb. capsulatus* exhibits a similar shift in redox potential (Stocker *et al.*, 1992) and similar effects have been observed for *Rb. sphaeroides* mutants (N. Woodbury, personal communication). The electroabsorption spectra of SYM-1 and (M)F195H are very similar to each other and to those of wild-type, except for a shift of the ΔA spectrum relative to A in the mutant. Note that, for wild-type, the minimum of ΔA is close to the maximum of A (c.f., Fig. 4). Aside from this shift, the magnitude and width of ΔA in the SYM-1 and (M)F195H mutants are essentially identical to those of wild-type (normalized to the absorbance at 800 nm, which is unaffected by the mutation). Although subtle, the shift of ΔA relative to A and its second derivative is a common feature in electroabsorption spectroscopy. Often the shift cannot be accounted for by a first derivative contribution because this distorts the relative contributions of the high- and low-energy sides of the electroabsorption spectrum. However, model calculations, following the suggestion of Middendorf *et al.* (1993) that the large $|\Delta\boldsymbol{\mu}_A|$ is caused by a specific interaction between the matrix field and a polarizable chromophore, indicate that such shifts may be caused by changes in the magnitude of the matrix field or in the relative energies of CT and exciton states. Both effects are likely to be present for these mutants. These subtle environmental effects on the electroabsorption of P may provide a further constraint on models for the electronic structure of P.

C. Other photosynthetic pigments

The effects of an applied electric field on the Q_Y absorption spectra of three antenna complexes from photosynthetic bacteria have been measured at 77 K (Gottfried *et al.*, 1991b): the Bchla protein (BCP) from *Prosthecochloris aestuarii*, the B800-850 light-harvesting complex from *Rb. sphaeroides*, and the B875 light-harvesting complex from *Rb. capsulatus*. For BCP in a glycerol/buffer glass, $|\Delta\boldsymbol{\mu}_A|$ for three of the resolved absorption bands was found to lie in the range 1.3-2.0 D/*f*. The electroabsorption line shape is well approximated by the second derivative of the absorption. This result is similar to that for monomeric Bchla embedded in a polymer film and for the 800-nm monomer Bchla band of *Rb. sphaeroides* RCs. Thus, the Bchla chromophores in BCP behave largely as a noninteracting set in an electric field. We emphasize that this does not imply that the chromophores interact weakly from the perspective of exciton interactions and energy transfer.

The factors that influence ΔA appear to require still stronger intermolecular interactions (as in P) combined with an asymmetric matrix electrostatic field. For B800-850 in a glycerol/buffer glass, the Bchla associated with the 800-nm band has a small $|\Delta\mu_A| = 0.8-0.9$ D/*f*, whereas the Bchla of the 850-nm band is found to have $|\Delta\mu_A| = 3.1-3.4$ D/*f*; however, the electroabsorption line shapes of both components are anomalous, which complicates the quantitative analysis. $|\Delta\mu_A|$ for the 850-nm band is nearly unchanged on attenuation of the 800-nm band by treatment with lithium dodecyl sulfate (LDS). The electroabsorption spectrum of the B875 complex was obtained in *Rb. capsulatus* whole chromatophore membranes from a strain that lacks B800-850. The line shape for B875 is also unusual, and the electroabsorption appears not to be dominated by a dipole moment change. Although very interesting in their own right, these data are useful because traces of antenna complexes sometimes contaminate RC preparations, especially of unstable mutants.

The effects of electric fields on the absorption spectra of the carotenoids spheroidene and spheroidenone in photosynthetic antenna and RC complexes (wild-type and several mutants) from purple nonsulfur bacteria have been compared with those for the isolated pigments in organic glasses (Gottfried *et al.*, 1991a,c]. In general, the field effects are substantially larger for the carotenoid in the protein complexes than for the extracted pigments and larger for spheroidenone than spheroidene. Further, the effects for carotenoids in all complexes are much larger than those for the Q_X transitions of the Bchl and Bphe pigments that absorb in the 450-700-nm spectral region. Quantitative analysis shows that the difference in the permanent dipole moment between the ground and excited state is substantially larger than for pure carotenoids extracted from the protein and studied in organic solvents. The latter exhibit large first derivative contributions to the ΔA line shape, that is, the electroabsorption is dominated by the change in polarizability. (Unlike the special pair, the carotenoids have the advantage that they can be extracted and studied separately, although there may be structural differences between *in vivo* and organic solvents.) These results demonstrate the presence of a large perturbation of the electronic structure of these nearly symmetric carotenoids, due to the organized environment in the protein. This experimental evidence provides a clear precedent for the model presented in the last section to explain $|\Delta\mu_A|$ for the special pair, once it is recognized that a molecular dimer is highly polarizable. The magnitude of the dipole moment change is found to be considerably larger in the B800-850 complex than in the RC for spheroidene, and is approximately equivalent in the two complexes for spheroidenone. These data provide a quantitative basis for the analysis of carotenoid bandshifts, which are used to measure transmembrane potential (e.g., Wraight *et al.*, 1978). Also, they highlight some of the pitfalls in making such measurements on complex membranes containing multiple populations of carotenoids.

Limited data have been presented for photosystem II (PSII) RCs (Lösche *et al.,* 1988). Analyzing the electroabsorption spectra for PSII is much more difficult because of the extensive overlap among the absorption bands in the Q_Y region and because of the uncertainty in the number of chromophores. The analysis by Lösche *et al.* (1988) used the PSII preparation of Nanba and Satoh (1987) in a PVA film. The authors suggest tentatively that $|\Delta\mu_A|$ for P680 is not much larger than for a monomeric Chla, in contrast to the special pair in bacterial RCs discussed in the previous section. We have repeated these measurements using the PSII preparation developed by Ghanotakis *et al.* (1989) and glycerol/buffer glasses, and find evidence that $|\Delta\mu_A|$ for the low-energy feature is considerably larger than for a monomeric Chla (Steffen, 1993). Unlike the bacterial RC, for which a very detailed analysis is possible, it is difficult to go much further with the analysis unless approaches can be found to clarify the absorption spectrum.

IV. Modulation of electron-transfer reaction rates

A. Principles

An electric field, F, changes the energy of a dipole moment as $\Delta U = -\boldsymbol{\mu} \cdot \mathbf{F}$. To put the magnitude in perspective, a single charge separated by 10 Å corresponds to a dipole moment of 50 D. The energy of this dipole aligned parallel or antiparallel to an electric field of 1 MV/cm is shifted by 100 meV. (1 MV/cm corresponds to a potential difference of 500 meV across a 50 Å lipid bilayer.) Both the initial and the final state of an electron transfer process can have dipole moments. The field interacts with the *difference* dipole moment, $\Delta\boldsymbol{\mu} = (\boldsymbol{\mu}_{\text{products}} - \boldsymbol{\mu}_{\text{reactants}})$. For charge separation reactions, $\boldsymbol{\mu}_{\text{products}} \gg \boldsymbol{\mu}_{\text{reactants}}$ so $\Delta\boldsymbol{\mu} \sim \boldsymbol{\mu}_{\text{products}}$; for charge recombination reactions, $\boldsymbol{\mu}_{\text{reactants}} \gg \boldsymbol{\mu}_{\text{products}}$ so $\Delta\boldsymbol{\mu} \sim \boldsymbol{\mu}_{\text{reactants}}$. All theories of electron transfer predict a significant dependence of the rate, k_{et}, on the change in free energy for the reaction (DeVault, 1984; Marcus and Sutin, 1985). Consequently, changing the rate of electron-transfer reactions with applied electric fields should be possible. In a sense, tuning the free energy by applying an electric field is equivalent to modifying the redox potential of the donor or acceptor, as has been demonstrated elegantly with numerous synthetic organic and inorganic model systems (Closs and Miller, 1988), by quinone substitution in the RC (Gunner *et al.,* 1986; Gunner and Dutton, 1989), and by changing the redox energies of P or H_L as described for several mutants in Section III,B. An important difference, which may have significant consequences for the RC system, is that an applied electric field also will affect the energy of dipolar states that are not actually populated, but that mediate the electron-transfer reaction by superexchange.

The goal of such studies is to obtain the dependence of the rate on free

energy in the vicinity of the zero-field free energy, to fit these results to models for electron-transfer reactions to obtain the parameters of interest, or to explore mechanistic issues such as the identity of intermediates or the origin of unidirectional electron transfer. Because the rates of many electron-transfer reactions in the RC are approximately independent of temperature, one expects at the outset that they are near the top of the rate vs. free energy curve. Consequently, the effect of an applied field will, for the most part, slow the electron-transfer rate. In a reaction network such as the RC, the situation may be much more complex, since level crossings may occur, opening new reaction channels that are absent at zero field. In such cases, unexpected deviations from standard electron-transfer theories would be observed for populations that are most perturbed by the field.

Although the effects of an applied electric field on the energies of dipolar states are conceptually simple, the field also may affect the electronic coupling between the initial and final state. Because the electronic coupling depends on the overlap of the wave functions of the donor and acceptor, the applied field may polarize the orbitals, changing the overlap. We are not aware of any experiments that address this issue directly; however, this effect is unlikely to be large under the field strengths available.

A second possibility, which is likely to play a significant role in RC electron-transfer reactions, is the effect of the field on mediating states. As will be discussed in Section IV,C in detail, the coupling between ^1P and P^+H^- has been suggested to involve superexchange via P^+B^- (Bixon *et al.*, 1987; Michel-Beyerle *et al.*, 1988; Plato *et al.*, 1988). Because the virtual state P^+B^- is also dipolar, its energy will change on application of a field. This energy is one of the critical determinants of the electronic coupling in theories of superexchange coupling. More precisely, the energy difference that enters the expression for the electronic coupling is the vertical energy between the crossing of the reactant and product surfaces (the transition state) and the mediating state surface. As the P^+H^- surface is shifted by application of a field, the nuclear coordinate of this crossing point changes. This effect is illustrated for the simplest one-dimensional potential surfaces in Fig. 8 (Boxer *et al.*, 1989). Because the dipole moment of a mediating state is roughly parallel to that of the final state (or the initial state for charge recombination), the potential surfaces for the dipolar product and mediating states will shift approximately in parallel. (Obviously the mediating state dipole is smaller and will shift less.) The combination of this roughly parallel shift and the change in the position of the transition state can, under certain circumstances, lead to the interesting situation that the energy denominator is approximately independent of field (note the approximate constancy of the lengths of the lines labeled $\Delta E_{13}(Q_{12})$ in Fig. 8). Consequently, the electronic coupling may be only weakly dependent on the applied field strength. This result also leads to the rather counterintuitive suggestion that the elec-

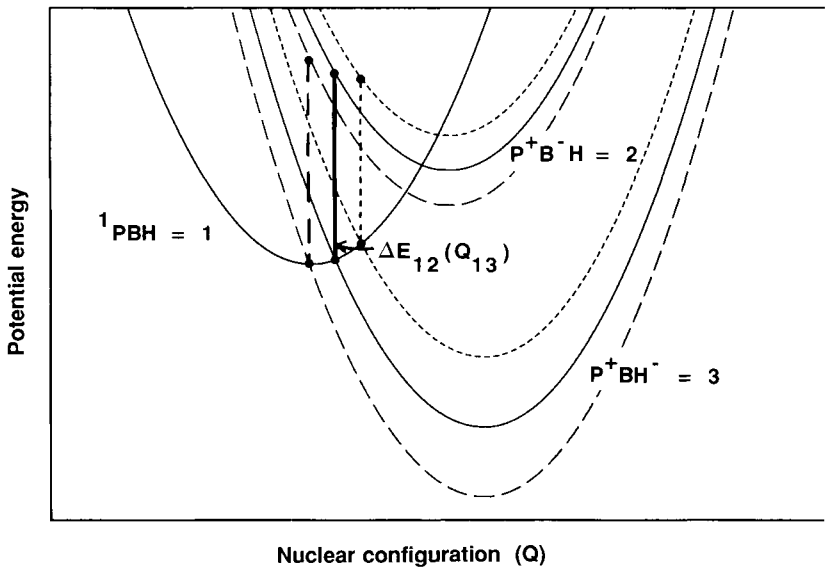

FIGURE 8 Schematic illustration of the relevant potential energy curves as a function of nuclear configuration for a superexchange mechanism for the initial electron transfer reaction in the RC (Boxer *et al.*, 1989; Lockhart *et al.*, 1990). State 1 ;= ^{1}P; state 2 = mediating state, for example, P^+B^- or ^{1}B; state 3 = P^+H^-. Zero-field curves (—) are given the effect of a field that is aligned (——) or opposed (---) to the permanent dipole moment of the final state is also shown (the dipole moment of state 1 is assumed to be negligible). Q_{13} is the value of Q at which the curves for the initial and final states cross along the relevant reaction coordinate (the transition state); $\Delta E_{12}(Q_{13})$ is the vertical energy difference between curves 1 and 2 at this value of Q_{13}. The interesting observation is that this vertical energy difference is only weakly dependent on applied field because the curves shift in parallel, leading to a shift in Q_{13}. As a result, for this configuration of surfaces, the dependence of the superexchange matrix element on applied field is expected to be quite weak (see also Franzen *et al.*, 1990).

tronic coupling may be much more strongly affected by an applied field if the mediating state is neutral, in which case these offsetting shifts are absent (Boxer *et al.*, 1989).

B. $P^+Q_A^-$ recombination reactions

The $P^+Q_A^-$ recombination reaction back to the neutral ground state is one of the best studied long-distance electron-transfer reactions in the RC. With the native ubiquinone (*Rb. sphaeroides*), the rate is approximately 20 sec^{-1} at room temperature and 39 sec^{-1} at low temperature (Kleinfeld *et al.*, 1984),

so kinetic data with extremely good signal-to-noise ratios can be obtained. Many different quinones have been substituted into the Q_A binding site (Gunner *et al.*, 1986; Gunner and Dutton, 1989). At least in a few cases, the approximate free energy of the $P^+Q_A^-$ state has been estimated by delayed fluorescence (Woodbury *et al.*, 1986). Curves based on theoretical electron-transfer models have been drawn through the kinetic data to extract information on the coupled vibrations. Among the interesting results that emerge is a surprisingly weak dependence of the recombination rate on temperature below 113 K for quite a wide range of free energies. For this result to occur a substantial fraction of the reorganization energy must involve coupling to high frequency modes (Gunner *et al.*, 1986). The $P^+Q_A^-$ recombination reaction can be quite complicated at higher temperatures, especially for quinones that are more difficult to reduce than ubiquinone (e.g., anthraquinone) because of a competing, thermally activated pathway that is likely to involve the intermediate $P^+H_L^-$, as described in detail by Kleinfeld *et al.* (1984). In the absence of an analysis at the level presented by Kleinfeld *et al.* (1984), it is difficult to know whether the apparent rates measured for many other quinones can be evaluated collectively in terms of electron-transfer theories for elementary processes.

The $P^+Q_A^-$ recombination reaction has been studied in applied electric fields at room temperature in planar lipid bilayers (Gopher *et al.*, 1985; Feher *et al.*, 1988) and in LB films (Popovic *et al.*, 1985,1986a,b). The results of these experiments were quite different, as discussed in detail by Feher *et al.* (1988). As shown in earlier work (Kleinfeld *et al.*, 1984), if Q_A is anthraquinone ($P^+Q_A^-$ energy about 100 meV higher than for ubiquinone; shown in Fig. 9), then activated recombination, presumably via P^+H^-, can occur. This possibility is evident in the bilayer experiments as the energy of $P^+Q_A^-$ is tuned closer to that of P^+H^- (the projection of the P^+H^- dipole on the director axis is substantially smaller than the $P^+Q_A^-$ dipole), leading to an increase in the decay rate, that was not observed by Popovic *et al.* (1985). Questions also were raised concerning the calibration of the field strength on the LB films. Feher *et al.* (1988) fit their data to a rate vs. free energy curve using a simple Marcus theory expression, but indicate that the fits are likely not to be unique.

We have studied the $P^+Q_A^-$ recombination reaction in PVA films at temperatures of 20 - 290 K (Franzen *et al.*, 1990; Franzen and Boxer, 1993). Because the RCs are not oriented, the field produces a spread in the free energies of dipolar states, making the analysis considerably more difficult than for an oriented sample. However, as shown in detail in Franzen *et al.* (1990), by measuring $P^+Q_A^-$ decay data with very good signal-to-noise over many $1/e$ times for many values of the applied field and by using relatively simple transformation methods, it is possible to extract reliably an experimental rate vs. free energy curve spanning a wide free energy range (more than 500 meV at 80 K). The method should be generally useful (Franzen *et al.*, 1992). The

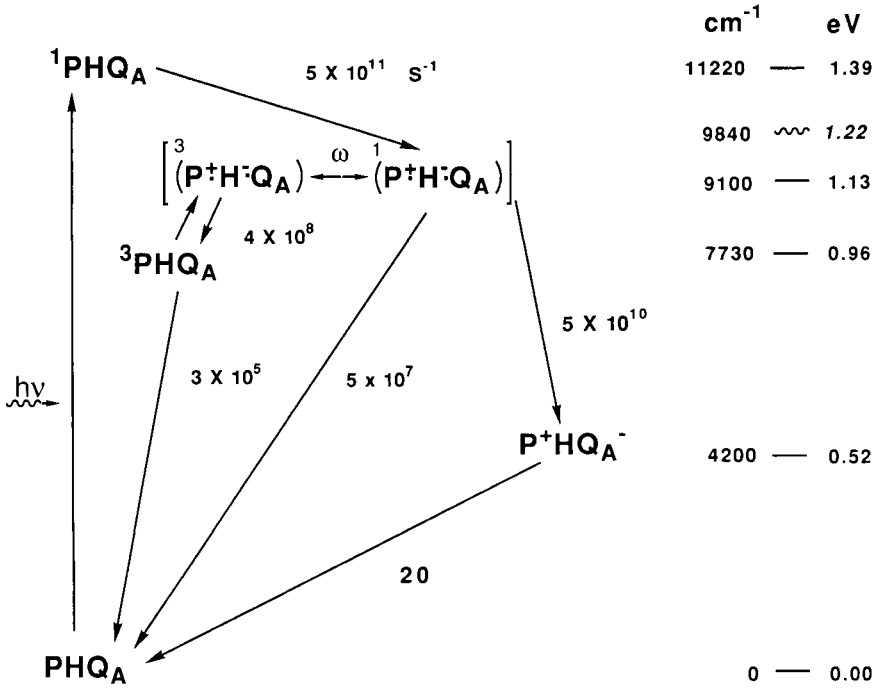

FIGURE 9 Reaction scheme and energy level diagram for the initial electron transfer reactions involving the components in Fig. 1. The energy of the P^+H^- state is especially important. The upper value (~) is obtained from delayed fluorescence measurements (Woodbury and Parson, 1984,1986) and the lower value from an analysis of activated recombination from the ^3P state (Goldstein *et al.*, 1988), the energy of which is known from phosphorescence measurements (Takiff and Boxer, 1988b). Nothing is known about the energy of the P^+B^- state except that it is above P^+H^-.

$P^+Q_A^-$ decay is biexponential at low temperature in frozen glasses (Shopes and Wraight, 1987; Sebban, 1988; Sebban and Wraight, 1989) and at all temperatures in PVA films. The origin(s) of this complication is not known, but may be related to the protonation state of the RC. Both the faster and slower decays were analyzed by Franzen *et al.* (1990), giving the rate vs. free energy curves shown in Fig. 10. Detailed methods for evaluating the error curves are presented in the original paper.

These experimental rate vs. free energy curves can be analyzed using various levels of electron-transfer theory to extract information on the modes that are coupled. For the faster process, good fits were obtained using a two-mode model; the total reorganization energy was divided approximately equally between a low and a high frequency mode with average frequencies of about 50 and 1500 cm^{-1}, respectively. Less satisfactory fits with roughly similar

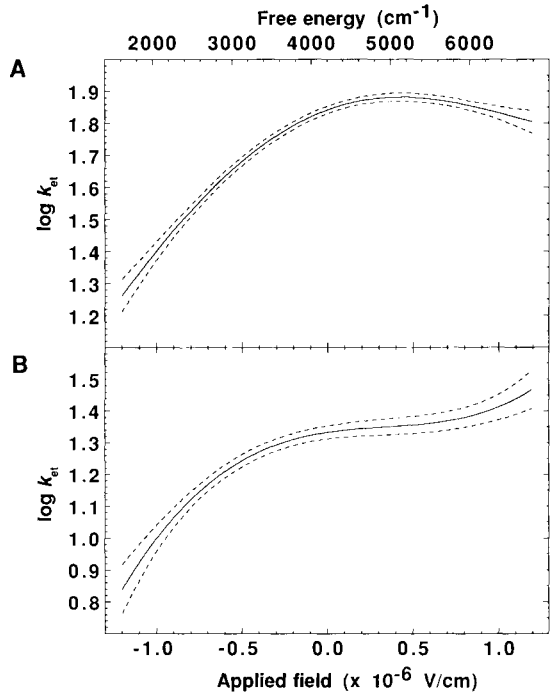

FIGURE 10 Experimental log k_{et} vs. ΔG curves for $P^+Q_A^-$ charge recombination obtained from an analysis of electromodulated decay curves at 80 K in poly(vinyl alcohol) (PVA) (Franzen *et al.*, 1990). The dotted curves above and below each curve represent the errors in the curve. These curves are continuous representations of the dependence of the rate on free energy, because an isotropic sample was used, giving a continuous distribution of free energies. The $P^+Q_A^-$ decay kinetics are biphasic at 80 K. Curves in A and B are for the fast and slow components, respectively.

parameters were obtained for the slower process. The upturn observed for the slower process at the largest driving force may be due to the onset of activated recombination via the P^+H^- state. With this information on the Franck-Condon factors, a detailed analysis of the electronic coupling was presented. The coupling between $P^+Q_A^-$ and the neutral ground state product at low temperature was shown to be consistent with superexchange involving the P^+H^- state (Franzen *et al.*, 1990). This result leads to a general model for back reactions in ordered sequential-electron-transfer systems such as the RC (Franzen *et al.*, 1993). At low temperature, each intermediate in the forward charge-separation direction can serve as the mediating state for back electron transfer from the next charge-separated state in the sequence; at high temperature, such intermediates are reformed during the activated

recombination from the next charge-separated state. By studying the effects of applied electric fields as a function of temperature or by modifying the redox properties (Kleinfeld *et al.*, 1984), these recombination pathways can be probed in detail. A very large acceleration of the decay is observed at room temperature in an applied electric field, along with interesting shifts in the steady-state population of the $P^+Q_A^-$ formed by the probe beam alone (Franzen and Boxer, 1993). The results at room temperature agree well with those of Feher *et al.* (1988) where they overlap. Because it is possible to control the timing, magnitude, and polarity of the applied field, a wide range of novel electric field effects can be explored and exploited.

C. Initial charge separation step: Fluorescence

Electric field effects have been used to investigate the initial $^1P \rightarrow P^+X^-$ reaction, where X is either B_L or H_L, by measuring the effect on the fluorescence that competes with this reaction (Lockhart and Boxer, 1988b; Lockhart *et al.*, 1988,1991; Ogrodnik *et al.*, 1990,1991), directly on the rate of formation of H_L^- (Lockhart *et al.*, 1990) and on the quantum yield of formation of P^+H^-, $P^+Q_A^-$, and ^3P (the latter in Q-depleted RCs) (Popovic *et al.*, 1986b; Moser *et al.*, 1988; Franzen, 1991; Boxer *et al.*, 1992; Ogrodnik *et al.*, 1992). To date, a considerable debate exists among ultrafast spectroscopists about the role of P^+B^- in the formation of P^+H^-, which all investigators agree is formed within about 3 ps of excitation of P at room temperature. This issue is discussed in detail in Chapters 3 - 5. Data supporting a two-step mechanism include those of Holzapfel *et al.* (1989,1990); data supporting a one-step formation of P^+H^- include those of Woodbury *et al.* (1985), Breton *et al.* (1988), and Kirmaier and Holten (1987,1988). Comparisons and limitations of the data are discussed in detail in Kirmaier and Holten (1991). The possibility that measurements of transient absorption may not be capable of distinguishing these mechanisms is discussed by Joseph and Bialek (1991). A combination of superexchange at low temperature and an activated two-step process at higher temperature has been proposed by Bixon *et al.* (1991) and some data have been analyzed in this context by Chan *et al.* (1992). This problematic situation suggests that alternative experimental approaches may be useful.

Central to any discussion of the mechanism of these initial reactions and the effects of temperature and applied electric fields on the rate is information on the energies of the states involved. The shapes of the potential surfaces are also crucial, but nothing is yet known directly from experiments about these shapes. In fact, very little information is available on the energies, aside from the energy of ^1P obtained from the absorption and fluorescence spectra (Woodbury and Parson, 1984,1986) and the ^3P energy, obtained from phosphorescence from ^3P (Takiff and Boxer, 1988a,b). The energy of P^+H^- has been estimated by measuring the delayed fluorescence amplitude associ-

ated with the activated reaction $P^+H^- \rightarrow {}^1P$ (Woodbury and Parson, 1984, 1986) and by measuring the free energy change associated with the back reaction ${}^3P \rightarrow P^+H^-$ (Chidsey *et al.*, 1984; Goldstein *et al.*, 1988). The results of these measurements are summarized with a reaction scheme in Fig. 9. The difference between the values obtained by the two types of measurements may be associated with the different time scales used to measure the effects. Evidence from delayed fluorescence suggests that the energy of P^+H^- (and presumably all other ion-pair states in the RC) relaxes in time (Woodbury and Parson, 1984,1986; Goldstein and Boxer, 1989a,b). One interesting difference is that the free energy change for the initial charge-separation step as measured by delayed fluorescence becomes very small as the temperature is lowered, whereas measurements of the decay of ${}^3P$ indicate that the free energy change is largely enthalpic. This difference may involve relaxation or solvation that is strongly temperature dependent.

Although neither experiment is without its limitations, the key result is that the driving force for the formation of P^+H^- is *at most* about 260 meV, and may be substantially less. If P^+B^- is formed as a real intermediate enroute to P^+H^-, then the driving force for this reaction must be smaller still. (Likewise, the driving force for the hypothetical $P^+B^- \rightarrow P^+H^-$ charge-shift reaction must be very small.) No experimental information is available on the P^+B^- energy. Free energy perturbation calculations suggest that $P^+B_L^-$ may be approximately isoenergetic with ${}^1P$, and $P^+B_M^-$ may be higher in energy (Parson *et al.*, 1990); however, the reported accuracy precludes more definitive statements. More recent calculations place P^+B^- much higher in energy (Marchi *et al.*, 1993). Thus, the free energy change for formation of P^+B^- is likely no greater than -100 meV and this state may lie higher in energy than ${}^1P$, which would preclude its rapid formation at low temperature. Also, the energy levels in the RC are unlikely to be very sharp. For example, the inhomogeneous linewidth of the lowest electronic transition of P is on the order of several hundred cm^{-1} (see Chapter 7). Thus, mechanisms that depend on a delicate balance among very precise values for the energies of the states or kinetic experiments that purport to derive such precise values should be viewed with caution.

The center-to-center separation of P and B is about 10 Å, leading to a 50-D dipole for P^+B^- if the charges are at the centers of the macrocycles. Unfortunately, no precise information is known about the distribution of charge on any of these radical ions on the time scale relevant to the analysis of the initial charge separation events. The very elegant and detailed EPR and ENDOR studies of P^+ and H_L^- are for the fully relaxed (solvated) ions, which may differ from the relevant charge distributions on the time scale of 1 ps. (No experimental information of any kind is available for B^-.) As discussed in detail by Lockhart and Boxer (1988b) and Lockhart *et al.* (1988), a reasonable approximation is to use the geometric center-to-center vector to estimate dipole moment strengths and directions. Ogrodnik *et al.* (1990,1991) have sug-

gested the use of P^+ charge distributions from an analysis of the spin density distribution measured in EPR/ENDOR experiments; however, no evidence exists that this approximation is better on the relevant time scale. These issues are critical because very large fields can be applied to RC samples, changing the energies of dipolar states by hundreds of meV if the dipole moments are on the order of 50 D or larger, as they must be within a few picoseconds once an electron moves from ^1P to H_L. Further, if the zero-field driving force is only on the order of 100 meV or less, then even a modest applied field can change the energy level separation in Fig. 9 by a large fraction. The mechanism and yields of the initial charge-separation steps will change in response to this change in energetics in an applied field.

As discussed in Section III,A, the effect of an applied electric field on the fluorescence spectrum should be the same as that for absorption. We were very surprised to discover that the actual effect on RC fluorescence was very different: the amplitude of the change is much larger and the line shape is dominated by an enhancement (zeroeth derivative effect) (Lockhart and Boxer, 1988a). As shown in Fig. 11, a small blue shift occurs without any change in linewidth. The χ dependence (fluorescence polarization induced by application of the applied field analyzed with a polarizer after the sample

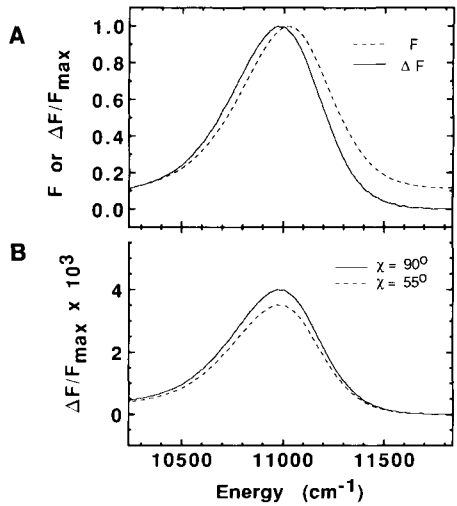

FIGURE 11 Effect of an applied field on the fluorescence spectrum of P (cf., the absorption effect in Figs. 4 and 6) (Lockhart *et al.*, 1991). A. Fluorescence spectrum of Q_A-depleted *Rb. sphaeroides* RCs in PVA at 77 K (---). Change in the fluorescence spectrum for the same sample with the experimental angle $\chi = 90°$ (—). The ΔF spectrum has been scaled to the same amplitude as the fluorescence spectrum to facilitate comparison of their shapes and positions. B. ΔF spectrum for an applied electric field of 1×10^5 V/cm with $\chi = 90°$ (—) and $\chi = 54.7°$ (---).

is excited isotropically) is shown in Figs. 5B and 11B and is very different from that in absorption. Our original interpretation of these results is that the field perturbs the rate of the initial electron-transfer reaction, which competes with fluorescence from ^1P. Because the reaction is approximately activationless, it is near the top of the rate vs. free energy curve, so the net effect of the field is to slow the initial step, increasing the fluorescence. Bixon and Jortner (1988) have analyzed the electric field effect data using a single low-frequency mode. This model (and semiclassical Marcus theory) predicts a much larger field effect than is observed because of the very strong dependence of the rate on driving force. The observation of a relatively weak effect suggests that the rate vs. free energy curve is much less steep, perhaps due to coupling to high-frequency modes (Boxer *et al.*, 1989; Lockhart *et al.*, 1990,1991).

The experiments were performed with Q-containing RCs at 77 K, at which temperature the contribution from delayed fluorescence to the steady-state signal should be small, at least at zero field. (Similar results were obtained with Q_A-depleted RCs; see subsequent text.) A potential problem with a steady-state fluorescence measurement is that a small, highly fluorescent, damaged population may dominate. [Note that, because the fluorescence is centered at about 920 nm, such a population, if it is present, has an intact special pair: measurements of the D_{LL} mutant, which lacks H_L, do not show the zeroeth derivative fluorescence increase seen for wild-type RCs (Boxer *et al.*, 1992).] This problem was checked by measuring the effect of a field on the rate of the initial charge-separation reaction by transient absorption spectroscopy, which is only sensitive to the bulk population (Lockhart *et al.*, 1990). At the highest fields available at the time (about 1 MV/cm), only a small reduction in the net rate was observed for the isotropic sample. To within a factor of 2, the directly measured integrated change in kinetics is consistent with the fluorescence electric field effect. If the intrinsic radiative rate of ^1P is several hundred ps [which is observed for the D_{LL} mutant that lacks H_L (Breton *et al.*, 1990)], then the large observed change in fluorescence on application of a field corresponds to only a small change in the rate of the initial step and is expected to be difficult to measure for an isotropic sample. If P^+B^- is being formed with a small driving force and its dipole moment is about 50 D, then $\Delta G(^1P \rightarrow P^+B^-)$ for a considerable fraction of the sample may be positive; much larger and more easily measured effects would have been expected. We conclude that dependence of the rate on ΔG is unusually weak.

No evidence was found for formation of H_M^- on application of the field (Lockhart *et al.*, 1990). The hypothetical $P^+B_L^-$ and $P^+B_M^-$ dipoles are approximately antiparallel; consequently, in those RC orientational subpopulations in which the $P^+B_L^-$ shifts to higher energy, the $P^+B_M^-$ shifts to lower energy and vice versa. If the energies of these states are similar and are related to unidirectional electron transfer (Parson *et al.*, 1990), one might expect

that, for those orientational subpopulations in which $P^+B_M^-$ is most lowered (and $P^+B_L^-$ is most raised), electron transfer down the M branch might occur. This effect was not observed. Note that for this type of experiment, it is essential to use a nonoriented sample.

The observation (Figs. 5B and 11B) that the fluorescence from ^1P is polarized upon application of an electric field even though the sample is isotropic and is excited isotropically is remarkable. The physical origin of this effect is related to the field effect itself. The shifting of the energy of dipolar states such as P^+H^- upon application of a field depends on the orientation of the dipole in the field. Because a shift in the energy of dipolar states changes the rate of electron transfer, different orientational subpopulations in the sample have different electron transfer rates. Because the changes in electron transfer rate are different for different orientational subpopulations, certain orientations will preferentially emit more fluorescence (those whose rates of forward electron transfer are slowed the most), while other orientational subpopulations will fluoresce less (those whose rate are increased). The result is that the fluorescence becomes polarized. Experimentally, ΔF is measured as a function of the angle χ between the applied field direction and the direction of the polarization in an analysing prism or polarized sheet. The connection with the RC molecular coordinates is as follows. Both the fluorescence transition dipole moment and the charge-separated dipole have well-defined and fixed orientations in the molecular axis system. The fluorescence transition moment direction can be measured by studying single crystals. The charge-separated dipole moment direction(s) can be estimated from the atomic coordinates of the RC (see below). For the case of the primary charge separation reaction, the likely charge-separated dipolar states whose formation might compete with fluorescence are the P^+P^- internal charge-transfer state of ^1P, P^+B^- and P^+H^- (the projections of these dipole moment directions on the transition dipole moment is about the same for the M- and L-branches). As discussed earlier, for an electron transfer reaction, what matters is the change in dipole moment, $\Delta\boldsymbol{\mu}_{et} = \boldsymbol{\mu}$(products) $-$ $\boldsymbol{\mu}$(reactants). It is straightforward to show (Lockhart *et al.*, 1988) that if the dependence of the rate on free energy can be expressed as a third order polynomial (as is the case for almost any physically reasonable rate vs. free energy curve), then ΔF depends on the experimental angle χ according to Eq. 2, where $\Delta\boldsymbol{\mu}_{et}$ replaces $\Delta\boldsymbol{\mu}_A$ and ζ_{et}, the angle between $\Delta\boldsymbol{\mu}_{et}$ and the fluorescence transition dipole moment replaces ζ_A. The data in Fig. 5B demonstrate that this form fits the observed χ-dependence.

The angle dependence is most striking, because the observed angle is very different from that for electronic excitation of P (cf. Fig. 5A,B). If the primary effect of the applied field is to change the rate of electron transfer that competes with fluorescence (as opposed to changing the rate of other nonradiative deactivation pathways), then the difference dipole moment that should

dominate the effect is $\Delta\boldsymbol{\mu}_{et} = \boldsymbol{\mu}(P^+X^-) - \boldsymbol{\mu}(^1P)$ for X = B or H. As discussed earlier, several uncertainties exist even in this simple expression. To the extent that the charge distribution in P^+ as it is initially formed is asymmetric relative to the geometric center of P, the charge distribution in ^1P is also likely to be asymmetric (Plato *et al.*, 1988). Then, taking the vector difference, this charge asymmetry cancels. This result is an additional justification for using the geometric center of P, a point that has been neglected in criticism by Ogrodnik *et al.* (1990,1991). No information on B^- is available and only limited data exist for H_L^-, so we (and Ogrodnik *et al.*, 1991) use the geometric centers. Thus, the directions of the P^+B^- and P^+H^- dipoles can be estimated largely based on the X-ray structure. The observable ζ_{et} is the angle between this dipole and the fluorescence transition dipole moment direction. This fluorescence transition moment direction is known approximately because the polarized absorption spectrum of a *Rps. viridis* RC single crystal has been reported (Zinth *et al.*, 1985), giving the direction of the absorption transition moment relative to the principle dichroic axes of the crystal. This information can be analyzed in terms of the molecular axis system using the X-ray coordinates. Early measurements of the angle between the fluorescence and absorption transition moments (Ebrey and Clayton, 1969) indicate that this angle is small (i.e., the moments are approximately parallel). With all these approximations in mind, the angle ζ_{et} (P^+B^-) was estimated to be about 49°, much less than the observed angle (Fig. 5B). $\zeta_{et}(P^+H^-)$ is estimated to be about 60°, closer to the observed angle. On this basis, we concluded that the dipole moment whose formation competes with fluorescence is not P^+B^-, so we favor a one-step mechanism. Our experiments have been extended significantly by Ogrodnik and co-workers (1991), who excited the RC using polarized light in the 500-600-nm region. Photoselection creates a small and somewhat selective anisotropy in the sample, depending on the chromophore that is excited (Raftery and Clayton, 1979). By encoding this additional information in the excitation beam, it is possible to distinguish more rigorously the rather small difference between $\zeta_{et}(P^+B^-)$ and $\zeta_{et}(P^+H^-)$. This refinement leads to a conclusion identical to that of our original experiment: that formation of the P^+B^- does not compete with the observed fluorescence.

The magnitude and field dependence of $\Delta F/F$ and the details of the line shape provide further constraints and support for the mechanism described earlier (Lockhart *et al.*, 1991). A surprisingly wide range of electric field modulated line shapes is possible because of the orientation-dependent competition between the electric field effect on the fluorescence spectrum and on the rate of electron transfer. One interesting result is that, because electron transfer occurs down the L side, the absolute direction of the $P^+H_L^-$ dipole is known. Analysis of the field and χ dependence of the ΔF line shape can provide information on the angle between $\Delta\boldsymbol{\mu}_F$ and this absolute direc-

tion. If the ground state dipole moment is small, then $\Delta\mu_F \sim \mu(^1P)$ and information can be obtained, in principle at least, on the direction of charge asymmetry in ^1P. The results are consistent with the negative end of the dipole (presumably the direction of incipient charge separation) on the M side Bchl of P. This chromophore is somewhat closer to B_L and H_L than is the L side Bchl of P (Plato *et al.*, 1988). The reader is referred to Lockhart *et al.* (1991) for the full details and approximations needed to reach this conclusion. The analytical methods provide the basis for analyzing the electric field modulated spectra of RC mutants with line shapes that are often quite unusual (Steffen, 1993), and applies equally well to the absorption line shapes of transient populations that are affected by fields (Lao *et al.*, 1993).

Several shortcomings are inherent in analyzing field effects on fluorescence. The most obvious is the possibility that only a minority population is detected. This possibility has been tested using RCs from several laboratories, many different preparations, several different species, and different media and by comparing results with those of direct kinetic measurements (Lockhart *et al.*, 1990). Any mechanism for the initial charge-separation step, especially the two-step mechanism involving initial formation of P^+B^-, leads to the expectation that the fluorescence should be modulated by an applied electric field, in fact, at least as much or more than we have observed. This and the fact that it is experimentally difficult to observe changes in transient absorption for isotropic samples whereas most models predict it should be readily detected are discussed in detail in Lockhart *et al.* (1990). The signal observed may be delayed fluorescence from that orientational subpopulation with P^+X^- dipoles that are aligned to raise the P^+X^- state close to ^1P. (Note that the prompt fluorescence from this orientational subpopulation also would be affected strongly.) Two observations argue against this explanation. First, a quadratic field dependence was obtained for Q_A-containing and Q_A-depleted RCs, with some deviation at the highest fields for Q_A-depleted RCs (Lockhart *et al.*, 1988c. The P^+H^- state is very short lived in Q_A-containing RCs; delayed fluorescence from the $P^+Q_A^-$ state is less likely in Q_A-containing RCs. Second, one might expect the field dependence of delayed fluorescence to be very strong, since the field enters into the exponent for activated recombination. An equation describing this superquadratic field dependence is given by Ogrodnik *et al.* (1991); however, the situation is more complex because the population that survives the initial step in a field (see Section IV,D) is the orientational subpopulation least affected by the field (i.e., the P^+X^- dipoles of the survivors that can give recombination fluorescence are more perpendicular than parallel or antiparallel to the field direction). The field dependence on this orientational subpopulation may be considerably weaker (Boxer *et al.*, 1992). These issues can be settled by measuring the field effect directly on the spontaneous fluorescence.

A further interesting complication arose in the course of these investiga-

tions (Boxer *et al.*, 1992). On prolonged irradiation of samples in PVA films at 77 K, the steady-state fluorescence was observed to increase and the ΔF signal changes sign (it has a negative zeroeth derivative line shape). Associated with this remarkable change is a reduction in the $P^+Q_A^-$ quantum yield (measured in the absence of a field). No systematic change is measured in the absorption, electroabsorption, or fluorescence line shapes, and there is no evidence for an increase in the triplet quantum yield (i.e., the reduction in the $P^+Q_A^-$ quantum yield is not due to accumulation of Q_A^-). All changes are reversible on warming the sample to room temperature. Although the underlying mechanism for this interesting phenomenon is not yet understood, it is critically important that any investigation of the fluorescence spectrum, its lifetime, and the electric field effect in PVA and at low temperature be performed under the lowest possible illumination. In the case of some RC mutants, this transformation occurs almost immediately in PVA (Boxer *et al.*, 1992).

Fluorescence electric field effects also have been reported for several antenna complexes: BCP, B800-850, and B875 (Gottfried *et al.*, 1991b). In all three antenna complexes, efficient energy transfer occurs from higher energy states to the lowest energy excited state and, at 77 K, fluorescence occurs primarily from this lowest state. The electric field modulated fluorescence of BCP shows nearly the same quantitative effect as that obtained from absorption, with $|\Delta\boldsymbol{\mu}_F| = 1.6$ D/*f*. In contrast, the B800-850 complex shows an unprecedented very large net decrease in fluorescence in an applied electric field. The mechanism for this novel effect is not understood. Some aspect of energy transfer or some other nonradiative decay pathway may depend on applied field. B875 also shows an electric field induced fluorescence decrease; however, the ΔF line shape is dominated by a first derivative contribution, not unlike the electroabsorption spectrum. An explanation for these results and others we have obtained for strongly interacting chromophores may lie in a breakdown of the standard treatments of electromodulation effects embodied in Eq. 1.

D. Initial charge separation step: Quantum yield failure

As discussed earlier, the fluorescence electric field effect may be complicated by several factors. Measuring the effects on the picosecond kinetics directly is quite difficult because the effects are small. We have investigated the effect of an applied electric field on the quantum yield and lifetime of all states whose lifetimes are greater than a few nanoseconds, including the quantum yields of P^+H^- and ^3P in Q_A-depleted RCs and $P^+Q_A^-$. The results at 80 K are summarized in Fig. 12 (Boxer *et al.*, 1992). The effect on the relative quantum yields of all three states is identical within experimental error. At the highest fields studied, nearly 3MV/cm, the effects are very large. A possibly related effect of a field on the $P^+Q_A^-$ quantum yield was observed earlier

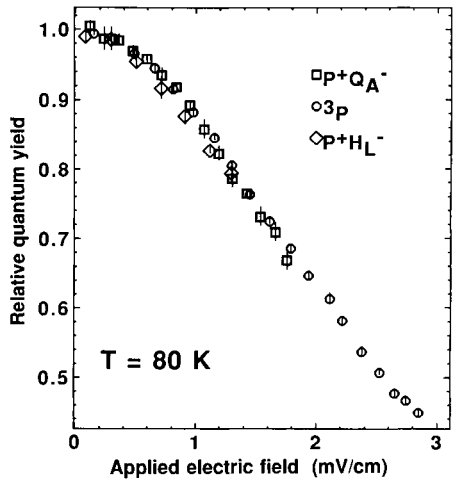

FIGURE 12 The effect of a large applied field on the relative quantum yield for formation of $P^+H_L^-$ (◇) and ^3P (○) in Q_A-depleted RCs and $P^+Q_A^-$ (□) in Q_A-containing RCs for *Rb. sphaeroides* RCs in dry PVA at 80 K (Franzen, 1991). The $P^+H_L^-$ quantum yield is measured ~10 ns after an exciting flash. The quantum yield for all three states decreases equally within the experimental error up to the highest field observed, suggesting that some state common to formation of all three intermediates is affected by the applied field.

by Popovic *et al.* (1986b) in LB films, and Ogrodnik *et al.* (1992) have recently reported similar results, over a narrow range of fields, for P^+H^- and $P^+Q_A^-$. The electric field is on during the formation of all three states (the slowest process is radical pair decay into ^3P). The field can be turned off prior to significant decay of $P^+Q_A^-$, so the concentration and decay of this population can be measured in the absence of a field. (The field affects both the $P^+Q_A^-$ decay rate, as discussed in Section IV,B, and the absorption spectrum of P, as discussed in Section III,B.) The field is on during both the formation and the decay of P^+H^- (~20 ns) and can be switched off prior to the decay of ^3P (~100 μs). We also have observed that the field has little effect on the P^+H^- decay rate (Franzen, 1991).

The implication of these results is that the electric field must be affecting some process prior to the decay of $P^+H^-Q_A$ into $P^+HQ_A^-$, and that any electric field effect on the decay of the triplet radical pair state into ^3P (rate constant k_T) or on the decay of $P^+H^-Q_A$ into $P^+HQ_A^-$ (rate constant k_Q) is not rate and, hence, not yield limiting. With reference to the reaction scheme in Fig. 9, the quantum yield of formation of all three states can be affected simultaneously in three ways: (1) the rate constant for formation of P^+H^- is retarded strongly by the applied field; (2) an electric field-dependent pathway exists for return to the ground state from ^1P or from another intermediate

prior to formation of P^+H^-; and (3) a field-dependent fraction of the initially formed P^+H^- recombines rapidly (<100 ps) to the ground state.

The intrinsic excited state lifetime of ^1P in the absence of electron transfer is not known. In the D_{LL} mutant in which H_L is removed, the ^1P stimulated emission decays in several hundred picoseconds (Breton *et al.*, 1990). If this is the radiative rate for ^1P in wild-type RCs, the observed electric field effect on the fluorescence from ^1P (measured up to 1 MV/cm), although causing an easily measurable change in the fluorescence quantum yield, implies a small change in the rate. This is consistent with the direct observation of the charge separation kinetics, also measured at a maximum field of 1 MV/cm and with the more limited signal-to-noise of picosecond decay experiments (Lockhart *et al.*, 1990). The quantum yield effects in Fig. 12 are considerably larger than these changes, so the first two possibilities listed earlier appear inconsistent with earlier data, with all the caveats outlined at the end of the last section and in the original papers. The third possibility implies that some aspect of the time evolution of the P^+H^- state in an electric field leads to a population loss to the ground state before the electron moves on to Q_A. As discussed earlier, delayed fluorescence measurements provide clear evidence that the free energy of the P^+H^- state relaxes on a very short time scale. On application of a field, the energy of the P^+H^- state for part of the sample is shifted considerably higher in energy. When the free energy of P^+H^- is higher (as in the β-mutant), the P^+H^- state could decay to an appreciable extent to the ground state, perhaps because the P^+B^- state can mediate this back reaction more efficiently (Kirmaier *et al.*, 1991). These observations suggest that part of the quantum yield failure for wild-type RCs in an applied field occurs for the orientational subpopulation with P^+H^- dipoles that are oriented to raise the P^+H^- energy, similar to the occurrence in the β-mutant in the absence of a field.

The population of RCs which undergoes quantum yield failure in an applied electric field and recovers rapidly to the ground state is not an isotropic population. Just as for the electric field induced fluorescence anisotropy discussed earlier, this is because different orientational subpopulations are shifted to a different extent in the field, and only certain ones experience quantum yield failure. The non-isotropic nature of the population that recovers quickly to the ground state can be probed either by measuring the χ-dependence of the absorption of the special pair (exactly analogous to the experiment in fluorescence, Fig. 5B), or it is possible to exploit the fact that the Stark effect spectrum of a non-isotropic distribution differs from an isotropic distribution (this is closely analogous to the field-induced fluorescence lineshapes described in detail in Lockhart *et al.*, 1991, see Fig. 11B). We have called the latter effect the dynamic Stark effect (Boxer *et al.*, 1992; Lao *et al.*, 1993). In principle, either measurement can provide information on the projection of the dipole moment associated with the state principally responsible

for quantum yield failure on the absorption transition dipole moment of P, whose orientation is known relative to the molecular axes (Zinth *et al.*, 1985). The data to date are inconsistent with states such as P^+P^- being responsible for quantum yield failure, but cannot yet distinguish between the P^+H^- and P^+B^- states.

The simplest explanation for the absence of a field effect on the decay of the P^+H^- state is that the orientational subpopulation that is most affected by whatever mechanism is responsible for the quantum yield failure has a dipole roughly parallel to the P^+H^- dipole. Because these dipoles are parallel or antiparallel to the applied field direction, the survivors, whose P^+H^- decay is measured, have P^+H^- dipoles roughly more perpendicular to and least affected by the field. In a sense, the applied field serves to filter orientational subpopulations. A possible additional mechanism may be that the rate-limiting process for decay of the P^+H^- state may not involve as large a change in dipole moment as expected and, therefore, may not be especially sensitive to the field. For example, if H^- were to protonate (i.e., form H·), and if deprotonation were rate limiting in the decay of $P^+H\cdot \rightarrow P^+H^- \rightarrow {}^3P$ or ground state, then the change in dipole moment would involve just the movement of a proton (e.g., a hydrogen-bonded proton). This change would be affected much less by a field than the change in dipole between P^+H^- and the ground state.

These simple suggestions can be tested by comparisons of measurements on many different time scales, at the highest possible fields, and for RC mutants for which the zero-field free energy change for the initial step is shifted relative to the wild-type. To date, these issues remain open. Because they relate to the mechanism(s) of the initial charge-separation step and the molecular basis for unidirectional electron transfer, electric field effects are likely to continue to be a useful tool.

Acknowledgments

I wish to thank the many students and postdoctoral fellows whose work is described in this chapter, including C. E. D. Chidsey, L. Takiff, Richard Goldstein, Robert Goldstein, D. J. Lockhart, T. R. Middendorf, D. S. Gottfried, S. Franzen, D. H. Oh, Ko-Q. Lao, L. Mazzola, S. L. Hammes, and J. W. Stocker. Preprints of work relevant to this review from D. Holten, C. C. Schenck, and J. Fajer are greatly appreciated. This work was supported by the NSF Biophysics Program.

References

Alegria, G., and Dutton, P. L. (1991a). *Biochim. Biophys. Acta* **1057**, 239.
Alegria, G., and Dutton, P. L. (1991b). *Biochim. Biophys. Acta* **1057**, 258.

Allen, J. P., Feher, G., Yeates, T. O., Komiya, H., and Rees, D. C. (1987). *Proc. Natl. Acad. Sci. U.S.A.* **84,** 5730.

Bixon, M., and Jortner, J. (1988). *J. Phys. Chem.* **92,** 7148

Bixon, M., Jortner, J., Michele-Beyerle, M., Ogrodnik, A., and Lersch, W. (1987). *Chem. Phys. Lett.* **140,** 622.

Bixon, M., Jortner, J., and Michel-Beyerle, M. E. (1991). *Biochim. Biophys. Acta* **1056,** 301-375.

Böttcher, C. J. F. (1973). "Theory of Dielectric Polarization." Vol. 1. Elsevier, Amsterdam.

Boxer, S. G. (1976). Ph.D. Thesis. University of Chicago, Illinois.

Boxer, S. G., and Closs, G. L. (1976). *J. Am. Chem. Soc.* **98,** 5406.

Boxer, S. G., Lockhart, D. J., and Middendorf, T. R. (1987). *Springer Proc. Phys.* **20,** 80.

Boxer, S. G., Goldstein, R. A., Lockhart, D. J., Middendorf, T. R., and Takiff, L. (1989). *J. Phys. Chem.* **93,** 8280.

Boxer, S. G., Lockhart, D. J., Kirmaier, C., and Holten, D. (1990). *In* "Perspectives in Photosynthesis" (J. Jortner and B. Pullman, eds.), p. 39. Kluwer Academic Publishers, Dordrecht, The Netherlands.

Boxer, S. G., Franzen, S., Lao, K., Lockhart, D. J., Stanley, R., Steffen, M., and Stocker, J. W. (1992). *In* The Photosynthetic Bacterial Reaction Center II. (J. Breton and A. Vermeglio, eds.), pp. 271-282. Plenum Press, New York.

Breton, J., Martin, J.-L., Migus, A., Antonetti, A., and Orszag, A. (1986). *Proc. Natl. Acad. Sci. U.S.A.* **83,** 5121.

Breton, J., Martin, J.-L., Fleming, G. R., and Lambry, J. C. (1988). *Biochemistry* **27,** 8276.

Breton, J., Martin, J.-L., Lambry, J.-C., Robles, S. J., and Youvan, D. C. (1990). *In* "Reaction Centers of Photosynthetic Bacteria" (M.-E. Michel-Beyerle, ed.), p. 293. Springer-Verlag, Berlin.

Bylina, E. J., and Youvan, D. (1988). *Proc. Natl. Acad. Sci. U.S.A.* **85,** 7226.

Chadwick, B. W., and Frank, H. A. (1986). *Biochim. Biophys. Acta* **851,** 257.

Chadwick, B. W., Zhang, C., Cogdell, R. J., and Frank, H. A. (1987). *Biochim. Biophys. Acta* **893,** 444.

Chance, B., and Smith, L. (1955). *Nature (London)* **175,** 803.

Chang, C. H., El-Kabbani, O., Tiede, D., Norris, J. R., and Schiffer, M. (1991). *Biochemistry* **30,** 5353.

Chidsey, C. E. D., Kirmaier, C., Holten, D., and Boxer, S. G. (1984). *Biochim. Biophys. Acta* **766,** 424.

Chan, C. K., Chen, L., DiMagno, T. J., Hanson, D. K., Nance, S. L., Schiffer, M., Norris, J. R., and Flemming, G. R. (1991). *Chem Phys. Lett.* **176,** 366.

Chan, C. K., DiMagno, T. J., Chen, L., Norris, J. R., and Fleming, G. R. (1991). *Proc. Natl. Acad. Sci. U.S.A.* **88,** 11202-11206.

Clayton, R. K., and Clayton, B. J. (1981). *Proc. Natl. Acad. Sci. U.S.A.* **78,** 5583.

Closs, G. L., and Miller, J. R. (1988). *Science* **240,** 440-446.

Cogdell, R. J., and Crofts, A. R. (1978). *Biochim. Biophys. Acta* **502,** 409.

Cogdell, R. J., and Frank, H. A. (1987). *Biochim. Biophys. Acta* **895,** 63.

Creighton, S., Hwang, J.-K., Warshel, A., Parson, W. W., and Norris, J. (1988). *Biochemistry* **27,** 774.

Dau, H. and Sauer, K. (1992). *Biochim. Biophys. Acta* **1102,** 91-106.

Davidsson, Å. (1980). *Chem. Phys.* **45,** 409-414.

Davidsson, Å., and Nordén, B. (1977). **10,** 447-454.

Davidsson, Å. (1983). *Chem. Phys. Lett.* **101,** 65-68.

de Grooth, B. G., and Amesz, J. (1977). *Biochim. Biophys. Acta* **462,** 237.

de Grooth, B. G., van Gorkum, H. J., and Meiburg, R. F. (1980). *Biochim. Biophys. Acta* **589,** 299.

Deisenhofer, J., Epp, O., Miki, K., Huber, R., and Michel, H. (1984). *J. Mol. Biol.* **180,** 385.

Deisenhofer, J., Epp, O., Miki, K., Huber, R., and Michel, H. (1985). *Nature (London)* **318,** 618.

DeLeeuv, D., Malley, M., Butterman, G., Okamura, M. Y., and Feher, G. (1982). *Biophys. Soc. Abstr.* **37,** 111a.

DeVault, D. (1984). "Quantum-Mechanical Tunneling in Biological Systems." Cambridge University Press, London.

DiMagno, T. J., Bylina, E. J., Angerhofer, A., Youvan, D. C., and Norris, J. (1990). *Biochemistry* **29,** 899.

Dutton, P. L., and Jackson, J. B. (1972). *Eur. J. Biochem.* **30,** 495.

Ebrey, T. G., and Clayton, R. K. (1969). *Photochem. Photobiol.* **10,** 109.

Fajer, J., Brune, D. C., Davis, M. S., Forman, A., and Spaulding, L. D. (1975). *Proc. Natl. Acad. Sci. U.S.A.* **72,** 4956.

Feher, G., Arno, T. R., and Okamura, M. Y. (1988). *In* "The Photosynthetic Bacterial Reaction Center: Structure and Dynamics" (J. Breton and A. Vermeglio, eds.), pp. 271-287. Plenum Press, New York.

Fleming, G. R., Martin, J.-L., and Breton, J. (1988). *Nature (London)* **333,** 190.

Frank, H. A., and Violette, C. A. (1989). *Biochim. Biophys. Acta* **976,** 222.

Frank, H. A., Chadwick, B. W., Taremi, S., Kolaczkowski, S., and Bowman, M. (1986). *FEBS Lett.* **203,** 157.

Franzen, S. (1991). Ph.D. Thesis. Stanford University, California.

Franzen, S., Goldstein, R., and Boxer, S. G. (1990). *J. Phys. Chem.* **94,** 5135.

Franzen, S., Lao, K., and Boxer, S. G. (1992). *Chem. Phys. Lett.* **197,** 380.

Franzen, S., and Boxer, S. G. (1993). *J. Phys. Chem.,* in press.

Franzen, S., Goldstein, R. F., and Boxer, S. G. (1993). *J. Phys. Chem.,* **97,** 3040.

Ghanotakis, D. F., de Paula, J. C., Demetriou, D. M., Bowlby, N. F., Petersen, J., Babcock, G. T., and Yocum, C. F. (1989). *Biochim. Biophys. Acta* **974,** 44.

Goldstein, R. A., and Boxer, S. G. (1989a). *Biochim. Biophys. Acta* **977,** 78.

Goldstein, R. A., and Boxer, S. G. (1989b). *Biochim. Biophys. Acta* **977,** 87.

Goldstein, R. A., Takiff, L., and Boxer, S. G. (1988). *Biochim. Biophys. Acta* **934,** 253.

Gopher, A., Schonfeld, M., Okamura, M. Y., and Feher, G. (1985). *Biophys. J.* **48,** 311-320.

Gottfried, D. S. (1990). Ph.D. Thesis. Stanford University, California.

Gottfried, D. S., and Boxer, S. G. (1992). *J. Lumin.* **51,** 39-50.

Gottfried, D. S., Steffen, M. A., and Boxer, S. G. (1991a). *Science* **251,** 662.

Gottfried, D. S., Stocker, J. W., and Boxer, S. G. (1991b). *Biochim. Biophys. Acta* **1059,** 63-75.

Gottfried, D. S., Steffen, M. A., and Boxer, S. G. (1991c). *Biochim. Biophys. Acta* **1059,** 76-90.

Gunner, M. R., and Dutton, P. L. (1989). *J. Am. Chem. Soc.* **111,** 3400.

Gunner, M. R., Robertson, D. E., and Dutton, P. L. (1986). *J. Phys. Chem.* **90,** 3783-3795.

Hammes, S. L., Mazzola, L., Boxer, S. G., Gaul, D. F., and Schenk, C. C. (1990). *Proc. Natl. Acad. Sci. U.S.A.* **87,** 5682.

Hanson, L. K., and Hofrichter, J. (1985). *Photochem. Photobiol.* **41,** 247.

Hanson, L. K., Fajer, J., Thompson, M. A., and Zerner, M. C. (1987). *J. Am. Chem. Soc. 109,* 4728.

Hochstrasser, R. (1973). *Acc. Chem. Res.* **6,** 263-269.

Holzapfel, W., Finkele, U., Kaiser, W., Oesterhelt, D., Scheer, H., Stilz, H. U., and Zinth, W. (1989). *Chem. Phys. Lett.* **160,** 1.

Holzapfel, W., Finkele, U., Kaiser, W., Oesterhelt, D., Scheer, H., Stilz, H. U., and Zinth, W. (1990). *Proc. Natl. Acad. Sci. U.S.A.* **87,** 5168.

Jackson, J. B., and Crofts, A. R. (1969). *FEBS Lett.* **4,** 185.

Jortner, J. (1980). *J. Am. Chem. Soc.* **102,** 6676.

Joseph, J., Bruno, W., and Bialek, T. (1991). *J. Phys. Chem.* **95,** 6242-6247.

Kirmaier, C., and Holten, D. (1987). *Photosynth. Res.* **13,** 225.

Kirmaier, C., and Holten, D. (1988). *FEBS Lett.* **239,** 211.

Kirmaier, C., and Holten, D. (1991). *Biochemistry* **30,** 609.

Kirmaier, C., Holten, D., Bylina, E. J., and Youvan, D. C. (1988). *Proc. Natl. Acad. Sci. U.S.A.* **85,**

7562.
Kirmaier, C., Gaul, D., DeBey, R., Holten, D., and Schenck, C. C. (1991). *Science* **251,** 922.
Kleinfeld, D., Okamura, M. Y., and Feher, G. (1984). *Biochemistry* **23,** 5780-5786.
Labhart, H. (1961). *Chimia* **15,** 20.
Lao, K., Franzen, S. F., Stanley, R., and Boxer, S. G. (1993). Submitted for publication.
Lin, S. H., Boeglin, A., Dai, H. L., and Schlag, E. W. (1988). *J. Phys. Chem.* **92,** 5398.
Liptay, W. (1974). *In* "Excited States" (E. C. Lim, ed.), Vol. 1, pp. 129-229. Academic Press, New York.
Liptay, W., and Czekalla, J. Z. (1960). *Z. Naturforsch.* **15,** 1072.
Liptay, W., Wortmann, R., Bohm, R., and Detzer, N. (1988). *Chem Phys.* **120,** 439.
Lockhart, D. J. (1989). Ph.D. Thesis. Stanford University, California.
Lockhart, D. J., and Boxer, S. G. (1987a). *Biochemistry* **26,** 664.
Lockhart, D. J., and Boxer, S. G. (1987b). *Biochemistry* **26,** 2958.
Lockhart, D. J., and Boxer, S. G. (1988a). *Proc. Natl. Acad. Sci. U.S.A.* **85,** 107.
Lockhart, D. J., and Boxer, S. G. (1988b). *Chem Phys. Lett.* **144,** 243.
Lockhart, D. J., Goldstein, R. F., and Boxer, S. G. (1988). *J. Phys. Chem.* **88,** 1408.
Lockhart, D. J., Kirmaier, C., Holten, D., and Boxer, S. G. (1990). *J. Phys. Chem.* **94,** 6987-6995.
Lockhart, D. J., Hammes, S. L., Franzen, S., and Boxer, S. G. (1991). *J. Phys. Chem.* **95,** 2217-2226.
Lösche, M., Feher, G., and Okamura, M. Y. (1987). *Proc. Natl. Acad. Sci. U.S.A.* **84,** 7537.
Lösche, M., Feher, G., and Okamura, M. Y. (1988). *In* "The Photosynthetic Bacterial Reaction Center—Structure and Dynamics" (J. Breton and A. Vermeglio, eds.), pp. 151-164. Plenum Press, New York.
Lo Surdo, A. (1913). Lincei Rend. **22,** J. Phys. Chem., in press.
McConnell, H. M. J. (1961). *Chem Phys.* **35,** 508-515.
McDowell, L. M., Gaul, D., Kirmaier, C., Holten, D., and Schenck, C. C. (1991). *Biochemistry* **30,** 8315-8322.
Malley, M. (1967). Ph.D. Thesis. University of California, San Diego.
Marchi, M., Gehlen, J., Chandler, D., and Newton, M. (1993). *J. Am. Chem. Soc.,* in press.
Marcus, R. A., and Sutin, N. (1985). *Biochim. Biophys. Acta* **811,** 265-322.
Mathies, R. A. (1974). Ph.D. Thesis. Cornell University, Ithaca, New York.
Mathies, R., and Stryer, L. (1976). *Proc. Natl. Acad. Sci. U.S.A.* **73,** 2169.
Matthews, B. W., Fenna, R. E., Bolognesi, M. C., Schmid, M. F., and Olson, J. M. (1979). *J. Mol. Biol.* **131,** 285.
Michel-Beyerle, M. E., Plato, M., Deisenhofer, J., Michel, H., Bixon, M., and Jortner, J. (1988). *Biochim. Biophys. Acta* **932,** 52.
Middendorf, T. R. (1991). Ph.D. Thesis. Stanford University, California.
Middendorf, T. R., Mazzola, J., and Boxer, S. G. (1991). *Biophys. J.* **59,** 139a.
Middendorf, T. R., Mazzola, L. T., Lao, K., Steffen, M., and Boxer, S. G. (1993). *Biochim. Biophys. Acta,* **1143,** 223-234.
Moser, C. C., Alegria, G., Gunner, M. R., and Dutton, P. L. (1988). *Israel J. Chem.* **28,** 133-139.
Nagaranjan, V., Parson, W. W., Gaul, D., and Schenck, C. (1990). *Proc. Natl. Acad. Sci. U.S.A.* **87,** 7888.
Nanba, O., and Satoh, K. (1987). *Proc. Natl. Acad. Sci. U.S.A.* **84,** 109.
Norris, J. R., DiMagno, T. J., Angerhofer, A., Chang, C. H., El-Kabbani, O., and Schiffer, M. (1990). *In* "Perspectives in Photosynthesis" (J. Jortner and B. Pullman, eds.), Vol. 22, pp. 11. Kluwer Academic Publishers, Dordrecht, The Netherlands.
Ogrodnik, A., Eberl, U., Heckmann, R., Kappl, M., Feick, R., and Michel-Beyerle, M. E. (1990). *In* "Reaction Centers of Photosynthetic Bacteria" (M. E. Michel-Beyerle, ed.), pp. 157. Springer-Verlag, Berlin.
Ogrodnik, A., Eberl, U., Heckmann, R., Kappl, M., Feick, R., and Michel-Beyerle, M. E. (1991). *J. Phys. Chem.* **95,** 2036-2041.

Ogrodnik, A., Laugenbacher, T., Bieser, G., Siegl, J., Eberl, U., Volk, M., Michel-Beyerle, M. E. (1992). *Chem Phys. Lett.* 198, 653-658.
Oh, D. H. (1991). Ph.D. Thesis. Stanford University, California.
Oh, D. H., and Boxer, S. G. (1990). *J. Am. Chem. Soc.* **112,** 8161.
Oh, D. H., Sano, M., and Boxer, S. G. (1991). *J. Am. Chem. Soc.* **113,** 6880-6890.
Parson, W. W., and Warshel, A. (1987). *J. Am. Chem. Soc.* **109,** 6152.
Parson, W. W., Creighton, S., and Warshel, A. (1988). *J. Phys. Chem.* **92,** 2696.
Parson, W. W., Creighton, S., and Warshel, A. (1989). *J. Am. Chem. Soc.* **111,** 4277.
Parson, W. W., Chu, Z. T., and Warshel, A. (1990). *Biochim. Biophys. Acta* **1017,** 251.
Plato, M., Möbius, K., Michel-Beyerle, M. E., Bixon, M., and Jortner, J. (1988). *J. Am. Chem. Soc.* **110,** 7279.
Ponder, M., and Mathies, R. (1983). *J. Phys. Chem.* **87,** 5090.
Popovic, A. D., Kovacs, G. J., Vincett, P. S., and Dutton, P. L. (1985). *Chem Phys. Lett.* **116,** 405-410.
Popovic, A. D., Kovacs, G. J., Vincett, P. S., Alegria, G., and Dutton, P. L. (1986a). *Chem Phys.* **110,** 227-237.
Popovic, A. D., Kovacs, G. J., Vincett, P. S., Alegria, G., and Dutton, P. L. (1986b). *Biochim. Biophys. Acta* **851,** 38-48.
Raftery, C. N., and Clayton, R. K. (1979). *Biochim. Biophys. Acta* **545,** 106.
Reimers, J. R., and Hush, N. S. (1991). *In* "Mixed-Valence Systems: Applications in Chemistry, Physics, and Biology" (K. Prassides, ed.), pp. 29-50. Kluwer Academic Publishers, Dordrecht, The Netherlands.
Robles, S. J., Breton, J., and Youvan, D. C. (1990a). *In* "Reaction Centers of Photosynthetic Bacteria" (M.-E. Michel-Beyerle, ed.), pp. 283, Springer-Verlag, Berlin.
Robles, S. J., Breton, J., and Youvan, D. C. (1990b). *Science* **248,** 1402.
Rodriguez, J., and Holten, D. (1989). *J. Chem. Phys.* **91,** 3525.
Schenck, C. C., Gaul, D. F., Steffen, M. A., Boxer, S. G., McDowell, L., Kirmaier, C., and Holten, D. (1990). *In* "Reaction Centers of Photosynthetic Bacteria" (M.-E. Michel-Beyerle, ed.), pp. 229. Springer-Verlag, Berlin.
Scherer, P. O. J., and Fischer, S. F. (1986). *Chem Phys. Lett.* **131,** 153.
Sebban, P. (1988). *Biochim. Biophys. Acta* **936,** 124.
Sebban, P., and Wraight, C. A. (1989). *Biochim. Biophys. Acta* **974,** 54.
Shopes, R. J., and Wraight, C. A. (1987). *Biochim. Biophys. Acta* **893,** 409.
Stark, J. (1913). *Ann. d. Phys.* **43,** 965.
Steffen, M. (1993). Ph.D. Thesis. Stanford University, California.
Stocker, J. W., Taguchi, A. K. W., Murchison, H. A., Woodbury, N. W., and Boxer, S. G. (1991). *Biochem.* **31,** 10356-10362.
Takiff, L., and Boxer, S. G. (1988a). *J. Am. Chem. Soc.* **110,** 4425.
Takiff, L., and Boxer, S. G. (1988b). *Biochim. Biophys. Acta* **932,** 325.
Thompson, M. A., Zerner, M. C., and Fajer, J. (1991). **95,** 5693-5700.
Trissl, H.-W., Breton, J., Deprez, J., and Leibl, W. (1987a). *Biochim. Biophys. Acta* **893,** 305.
Trissl, H.-W., Leibl, W., Deprez, J., Dobek, A., and Breton, J. (1987b). *Biochim. Biophys. Acta* **893,** 320.
Vincett, P. S., and Roberts, G. G. (1980). *Thin Solid Films* **68,** 135.
Vos, M. H. (1988). Ph.D. Thesis. University of Leiden, The Netherlands.
Vos, M. H., and van Gorkom, H. J. (1988). *Biochim. Biophys. Acta* **934,** 293.
Warshel, A., and Parson, W. W. (1987). *J. Am. Chem. Soc.* **109,** 6143.
Warshel, A., Creighton, S., and Parson, W. W. (1988). *J. Phys. Chem.* **92,** 2696.
Won, Y., and Friesner, R. A. (1988a). *J. Phys. Chem.* **92,** 2214.
Won, Y., and Friesner, R. A. (1988b). *Biochim. Biophys. Acta* **935,** 9.
Woodbury, N. W., and Parson, W. W. (1984). *Biochim. Biophys. Acta* **767,** 345.
Woodbury, N. W., and Parson, W. W. (1986). *Biochim. Biophys. Acta* **850,** 197.

Woodbury, N. W., Becker, M., Middendorf, D., and Parson, W. W. (1985). *Biochemistry* **24,** 7516.

Woodbury, N. W., Parson, W. W., Gunner, M. R., Prince, R. C., and Dutton, P. L. (1986). *Biochim. Biophys. Acta* **851,** 6.

Woodbury, N. W., Taguchi, A. K., Stocker, J. W., and Boxer, S. G. (1990). *In* "Reaction Centers of Photosynthetic Bacteria" (M.-E. Michel-Beyerle, ed.), pp. 303, Springer-Verlag, Berlin.

Wortmann, R., Elich, K., and Liptay, W. (1988). *Chem. Phys.* **124,** 395.

Wraight, C. A., and Clayton, R. K. (1973). *Biochim. Biophys. Acta* **333,** 246–260.

Wraight, C. A., Codgell, R. J., and Chance, B. (1978). *In* "The Photosynthetic Bacteria" (R. K. Clayton and W. R. Sistrom, eds.), pp. 471. Plenum Press, New York.

Youvan, D. C., Ismail, S., and Bylina, E. J. (1985). *Gene* **38,** 19.

Zinth, W., Sander, M., Dobler, J., and Kaiser, W. (1985). *In* "Antennas and Reaction Centers of Photosynthetic Bacteria" (M. E. Michel-Beyerle, ed.) Vol. 42, pp. 97–102. Springer-Verlag, Berlin.